**Mathematical Biology**

# Spatial movement with distributed memory

Qingyan Shi[1] · Junping Shi[2] (iD) · Hao Wang[3] (iD)

## Abstract

Diffusion has been widely applied to model animal movement that follows Brownian motion. However, animals typically move in non-Brownian ways due to their perceptual judgment. Spatial memory and cognition recently have received much attention in characterizing complicated animal movement behaviours. Explicit spatial memory is modeled via a distributed delayed diffusion term in this paper. The distributed time represents the memory growth and decay over time, and the spatial nonlocality reflects the dependence of spatial memory on location. When the temporal delay kernel is weak under the assumption that animals can immediately acquire knowledge and memory decays over time, the equation is equivalent to a Keller–Segel chemotaxis model. For the strong kernel with learning and memory decay stages, rich spatiotemporal dynamics, such as Turing and checker-board patterns, appear via spatially non-homogeneous steady-state and Hopf bifurcations.

✉ Junping Shi
   jxshix@wm.edu

   Qingyan Shi
   qingyanshi@jiangnan.edu.cn

   Hao Wang
   hao8@ualberta.ca

[1] School of Science, Jiangnan University, Wuxi 214122, Jiangsu, China

[2] Department of Mathematics, William & Mary, Williamsburg, VA 23187-8795, USA

[3] Department of Mathematical and Statistical Sciences, University of Alberta, Edmonton, AB T6G 2G1, Canada

🖄 Springer

# 1 Introduction

The diffusion equation has been popularly used to model random movements of both macroscopic and microscopic substances. Though, in general, diffusion has an averaging and smoothing effect on the distribution of the density function, different diffusion rates of different species may lead to spatial pattern formation as a result of Turing instabilities (Turing 1952). However, animal movement usually follows non-Brownian motion in nature. For instance, there are some kinds of biased animal movement in predator-prey systems: the prey-taxis or predator-taxis effect (Kareiva and Odell 1987; Lee et al. 2009; Wu et al. 2016; Tao 2010) which describes the repulsive or attractive animal movement due to the fear of the predation risk or the attraction of a predator to prey. These examples all ignore the delay effect caused by the memory of animals. Recently, it has been recognized that spatial memory and cognition are important factors for determining animals' diffusive movement with bias (Fagan et al. 2013).

Cognitive processes play a significant role in animals' movement decisions, and animal movement modeling can be complicated because of different perceptual mechanisms (Golledge 1998; O'Keefe and Nadel 1978). Although specific mechanisms are still debatable, most modelers believe that perception (information acquisition) and memory (the retention of information) play dominant roles in interpreting complicated animal movement behaviors. Generally speaking, memory is the storage, encoding, and recalling of information. Spatial memory is the memory of spatial locations in a living organism landscape. A strong motivation for the significance of spatial memory in animal movements is the empirical evidence of blue whale migrations presented by Abrahms et al. (2019) and discussed by Fagan (2019). Much progress has been made in incorporating spatial cognition or memory implicitly, such as home range analysis (Moorcroft et al. 1999; Moorcroft and Lewis 2006), scent marks (Lewis and Murray 1993), taxis-driven pattern formation (Potts and Lewis 2019, 2016), information gaining through the last visit to locations (Schlägel and Lewis 2014), perceptual ranges (Fagan et al. 2017), and delayed resource-driven movement (Foss-Grant 2017). Among these models, the closest one to ours is the model proposed in Potts and Lewis (2019), where there is a drift term depending on the spatially averaged population density at the current time. The model was used to study territorial pattern formation in Potts and Lewis (2016). However, this model ignores the delay effect induced by spatial memory. In Schlägel and Lewis (2014), the authors demonstrated that animals may gain information through the last visit to locations. Moreover, they explored the movement patterns induced by the interactions of information gained via past visits and environmental information. Fagan et al. (2017) proposed a resource-driven movement model for studying perceptual ranges and foraging success, and the delay effect was later considered in the resource-driven movement model in Foss-Grant (2017).

We formulate a partial differential equation model for a single species animal movement with the explicit incorporation of spatial memory via a distributed spatiotemporal delayed diffusion. Throughout the paper, we use $u(x, t)$ to denote the population density of species in spatial location $x$ at time $t$. It is also assumed that the population is in

a spatial habitat $\Omega$, an open, bounded, and connected subset of $\mathbb{R}^m$ with $m = 1, 2, 3$. The boundary $\partial\Omega$ is smooth. Then, the population density $u(x, t)$ satisfies

$$
\begin{cases}
u_t(x, t) = d_1 \Delta u(x, t) + d_2 div(u(x, t)\nabla v(x, t)) + f(u(x, t)), & x \in \Omega, \ t > 0, \\
\partial_n u(x, t) = 0, & x \in \partial\Omega, \ t > 0, \\
u(x, t) = \eta(x, t), & x \in \Omega, \ t \in (-\infty, 0],
\end{cases}
\tag{1.1}
$$

where the function $v(x, t)$ is defined by

$$
v(x, t) = g * G * u(x, t) = \int_{-\infty}^{t} \int_{\Omega} G(x, y, t - s)g(t - s)u(y, s)dyds. \tag{1.2}
$$

Here the parameters $d_1 > 0$ and $d_2 \in \mathbb{R}$ are the random diffusion coefficient and the memory-based diffusion coefficient, respectively; the function $f$ describes the biological birth/death of the population; the function $u(x, t)$ satisfies a Neumann type boundary condition $\partial_n u(x, t) = 0$ ($\partial_n u$ is the outer normal derivative of $u$ at $x \in \partial\Omega$), which makes the system mass-preserved with properly chosen kernel function $G$; and $\eta(x, t) \geq 0$ is the initial condition.

In this model, the memory-based distribution function $v(x, t)$ depends on time and location, as we assume that animals have knowledge of their prior spatial distributions from knowledge transfer, which is different from the assumption in Schlägel and Lewis (2014) that the information gaining comes from past visiting experiences. In (1.2), the spatial weighting function $G(x, y, t)$ measures the familiarity of the animals at location $y$ for the environmental information of location $x$ and describes how the accumulated information in animals' mind depends on space. Here we choose the Green's function of the diffusion equation with homogeneous Neumann boundary condition as the spatiotemporal kernel function $G(x, y, t)$, which preserves the biomass. From the boundary condition that $\partial_n G(x, \cdot, t) = 0$ where $\partial_n G(x, \cdot, t)$ is the outer normal derivative of $G$ with respect to $x$, one can obtain that $\partial_n v(x, t) = 0$ holds for $x \in \partial\Omega$. Together with $\partial_n u(x, t) = 0$, we have $d_1 \partial_n u(x, t) + d_2 u(x, t)\partial_n v(x, t) = 0$ on the boundary of $\Omega$. Hence the Neumann boundary condition in (1.1) is equivalent to a no-flux boundary condition for $u$. Under the above assumption, we have

$$
G(x, y, t) = \sum_{j=0}^{\infty} e^{-d_1 \lambda_j t} \phi_j(x)\phi_j(y), \tag{1.3}
$$

where $\lambda_j$ satisfying $0 = \lambda_0 < \lambda_1 \leq \lambda_2 \leq \cdots \leq \lambda_j \leq \cdots \to +\infty$, as $j \to \infty$, are the eigenvalues of the eigenvalue problem

$$
\begin{cases}
-\Delta\phi(x) = \lambda\phi(x), & x \in \Omega, \\
\partial_n\phi(x) = 0, & x \in \partial\Omega,
\end{cases}
\tag{1.4}
$$

and $\phi_j(x)$ are the normalized corresponding eigenfunctions of $\lambda_j$. Equivalently, the function $G(x, y, t)$ satisfies (for fixed $y$)

$$\begin{cases} G_t(x, y, t) = d_1 \Delta_x G(x, y, t), & x \in \Omega, \ t > 0, \\ \partial_n G(x, y, t) = 0, & x \in \partial\Omega, \ t > 0, \\ G(x, y, 0) = \delta(x - y). \end{cases}$$

Here $\delta(x)$ is the Dirac delta measure on $\Omega$.

The temporal weighting function $g(t)$ shows the distribution of memory dependence on the past time. In our model, we choose the Gamma distribution function of order $k$ (with $k \in \mathbb{N} \cup \{0\}$):

$$g_k(t) = \frac{t^k e^{-t/\tau}}{\tau^{k+1} \Gamma(k+1)}. \tag{1.5}$$

In particular, we mainly consider the following two specific cases which are commonly employed in the biological modeling (Cooke and Grossman 1982; Gourley and Ruan 2000; Macdonald 1987):

$$g_0(t) = g_w(t) = \frac{1}{\tau} e^{-\frac{t}{\tau}}, \quad g_1(t) = g_s(t) = \frac{t}{\tau^2} e^{-\frac{t}{\tau}}. \tag{1.6}$$

These are referred to as the weak kernel and the strong kernel, respectively. The weak kernel function $g_w(t)$ is strictly decreasing in $t$, which biologically reflects one of the common ways of memory decay: the longer time goes by, the dimmer memories become. While the strong kernel $g_s(t)$ is increasing first and then decreasing, which indicates the knowledge acquisition phase and the knowledge decay phase. The mean and variance of $g_j(\cdot)$ are given by $\mathbb{E}(g_j(\cdot)) = (j+1)\tau$ and $\mathbb{V}ar(g_j(\cdot)) = (j+1)\tau^2$, both of which depend on $\tau$, hence $\tau$ is related to the average of delay kernels. In this sense, we take $\tau$ as the parameter to measure the influence of spatial memory on the dynamics.

Moreover, $G : \Omega \times \Omega \times (0, \infty) \to \mathbb{R}^+$ is a (generalized) measure and $g : [0, \infty) \to \mathbb{R}^+$ is a probability distribution function satisfying

$$\int_\Omega G(x, y, t)dx = 1, \quad y \in \Omega, \ t > 0, \quad \text{and} \quad \int_0^\infty g(t)dt = 1. \tag{1.7}$$

Hence the function $v(x, t)$ is a spatiotemporal average of the past population density, and it is reasonable to call $v(x, t)$ the memory function of the population. In the model (1.1), we also assume that while moving around, animals collect information about the global situation with the spatial weighting function $G$ (knowledge depending on space) and the temporal weighting function $g$ (knowledge growth and decay over time); at their current position, the gradient of the past accumulated weighted spatial information of the population serves as the velocity in the advection term; and apart from advection, the random diffusion term describes the unbiased motion of animals. Similar to the classical diffusion equation, the model (1.1) describes the average behavior of all individuals in a group by ignoring individual behaviors.

The movement of population in (1.1)–(1.2) can be derived from mass conservation law and a modified Fick's law following Shi et al. (2020):

$$\mathbf{J}(x,t) = -d_1 \nabla_x u(x,t) - d_2 \mathbf{w}(x,t) \cdot u(x,t),$$

where $\mathbf{w}(x,t)$ is a vector field indicating animal movement direction and strength. In (1.1), we assume that

$$\mathbf{w}(x,t) = \nabla_x \left( \int_{-\infty}^{t} \int_{\Omega} G(x,y,t-s)g(t-s)u(y,s)dyds \right). \qquad (1.8)$$

In addition to the random diffusion with the coefficient $d_1$, the flux is proportional to the negative gradient of a weighted average historic density distribution. In Shi et al. (2020) and Shi et al. (2019), it is assumed that

$$\mathbf{w}(x,t) = \nabla_x u(x,t-\tau),$$

which indicates the flux is proportional to the negative gradient of historic density function at a fixed past time. However, it is more realistic to use a nonlocally and temporally distributed average of spatial memory because the temporal and spatial distributed delay reflects that the decay of spatial memory depends on time and the distance of past animal distributions from the decision-making individual. Such nonlocal delay $v(x,t)$ defined in (1.2) was first used in Britton (1990) for an unbounded domain and in Gourley and So (2002) for a bounded domain, see also (Chen and Yu 2016; Zuo and Song 2015; Zuo and Shi 2021) for related work. In all existing work, the nonlocal delay always appears in the reaction term (growth, etc.) of the population, while in our model (1.1), the nonlocal delay appears in the diffusion term of the population. Eq. (1.8) represents a nonlocal flux, and another type of nonlocal advection effect is considered in (Ducrot et al. 2018; Hillen and Buttenschön 2020) but for a totally different context.

In this paper the dynamic properties and pattern formation mechanisms of (1.1)–(1.2) are extensively studied via bifurcation analysis. To be more specific, we provide the conditions on the diffusion coefficients $d_1, d_2$ and the kernel functions for the spatial patterns (non-constant steady states) or spatiotemporal patterns (spatially non-homogeneous time periodic orbits) to be generated by the system (1.1)–(1.2). When the spatiotemporal kernel function $G(x,y,t)$ is given by (1.3) and the delay-dependent kernel function $g(t)$ is given by (1.6), system (1.1)–(1.2) is equivalent to a system of reaction–diffusion equations with a chemotactic term (Gourley and So 2002; Zuo and Shi 2021). For example, with the weak kernel $g_w(t)$, the equation of $u$ in (1.1) with $v$ given by (1.2) is equivalent to a system of two reaction–diffusion equations:

$$\begin{cases} u_t(x,t) = d_1 \Delta u(x,t) + d_2 div(u(x,t)\nabla v(x,t)) + f(u(x,t)), & x \in \Omega, \ t > 0, \\ v_t(x,t) = d_1 \Delta v(x,t) + \frac{1}{\tau}(u(x,t) - v(x,t)), & x \in \Omega, \ t > 0, \\ \partial_n u(x,t) = \partial_n v(x,t) = 0, & x \in \partial\Omega, \ t > 0. \end{cases} \qquad (1.9)$$

Our theoretical results on the pattern formation are mainly derived from the bifurcation theory for the equivalent system (1.9) and the corresponding one for the strong kernel. It is also a surprising coincidence that system (1.9) is the same as a rescaled Keller–Segel chemotaxis model with growth (Bellomo et al. 2015; Hillen and Painter 2009; Keller and Segel 1970; Tello and Winkler 2007):

$$
\begin{cases}
u_t(x,t) = d_1 \Delta u(x,t) + d_2 div(u(x,t)\nabla v(x,t)) + f(u(x,t)), & x \in \Omega, \ t > 0, \\
v_t(x,t) = d_3 \Delta v(x,t) + au(x,t) - bv(x,t), & x \in \Omega, \ t > 0, \\
\partial_n u(x,t) = \partial_n v(x,t) = 0, & x \in \partial\Omega, \ t > 0.
\end{cases}
$$
(1.10)

Typically $u(x,t)$ in (1.10) is the population density of cells, and $v(x,t)$ is the density of a chemical signaling molecule. In model (1.10), $d_1$ and $d_3$ are the random diffusion rates for $u$ and $v$ respectively, $d_2$ is the biased taxis-driven diffusion rate, $a$ and $b$ are the rates of production and degradation of the chemical signal $v$ (Hillen and Painter 2009). When the growth function $f(u) = 0$, Eq. (1.10) is the so-called minimal Keller–Segel model proposed by the seminal work of Keller and Segel (1970). The dynamics of (1.10) with growth rate has been studied in, for example, (Winkler 2010, 2014b, a, 2017). The chemotaxis coefficient $d_2$ in the original Keller–Segel model is negative since cells are usually attracted to the chemical signals' higher density location. Still, the repulsive chemotaxis effect (with positive $d_2$) has also been considered (Tao 2013; Wang and Zhao 2013). The above discussion provides an alternative derivation of the Keller–Segel chemotaxis model, but the variable $v$ is now interpreted as the "memory" which is a nonlocal and temporal distributed average of historic densities, instead of as a current chemical signaling function in the classical Keller–Segel model. On the other hand, our new model based on nonlocal delayed memory can also be understood as a chemotaxis model in which the population is either attracted to ($d_2 < 0$) or repelled by ($d_2 > 0$) its past tracks (Shi et al. 2020). Naturally, animals escape from high density due to the limitation of resources. Thus the animals will flee from the high-density area in their memory, so we have $d_2 > 0$. However, some social animals have aggregations, such as starling flocks and insects, for group defense or group working (van Schaik 2010; Kappeler 2010). Such group behavior will impel the animals to be attracted to the high-density area, which leads to $d_2 < 0$. Potentially, some animals may use optimal mixed strategies of social behaviors according to the environmental conditions. For instance, they may select to move to location with higher density where resources are abundant, and they need to work together, but they may select to move to location with lower density next time when resources are limiting. In this case, we have the switching between $d_2 > 0$ and $d_2 < 0$ when some environmental conditions change. However, we shall not consider such generalizations here, and for simplicity, we focus on pure strategies where $d_2$ attains a constant.

Throughout the paper, we assume that the nonlinear function $f$ and diffusion coefficients satisfy

(H1) $f : U \to \mathbb{R}$ is continuously differentiable, where $U$ is an open interval; and there exists $\theta \in U$ such that $f(\theta) = 0$ and $f'(\theta) < 0$;

(H2) $d_1 > 0, d_2 \in \mathbb{R}$.

Our main interest is the stability of the constant equilibrium $u = \theta$ with respect to (1.10) (or the equivalent system), and the instability often leads to the existence of spatial or spatiotemporal patterns. Our main results can be summarized as follows:

1. for the weak kernel case: there exists $d_2^* < 0$ such that the constant equilibrium is locally asymptotically stable when $d_2 \geq d_2^*$, and it is unstable when $d_2 < d_2^*$. Moreover steady-state bifurcations occur at a sequence of values $d_2 = d_{2,n}^w$ ($\leq d_2^*$) to give rise to spatial patterns;

2. for the strong kernel case: there exist $d_{2,S}^* < 0$ and $d_{2,H}^* > 0$ such that

   (a) when $d_{2,S}^* \leq d_2 \leq d_{2,H}^*$, the constant equilibrium is locally asymptotically stable;

   (b) when $d_2 > d_{2,H}^*$, the constant equilibrium is unstable, and a family of Hopf bifurcations occur at a sequence of values $d_2 = d_{2,n}^H$ ($\geq d_{2,H}^*$) and spatially non-homogeneous periodic orbits arise;

   (c) when $d_2 < d_{2,S}^*$, the constant equilibrium is unstable, and a family of steady-state bifurcations occur at $d_2 = d_{2,n}^S$ ($\leq d_{2,S}^*$) and spatially non-homogeneous steady states arise.

These results are similar to diffusion-induced Turing instability in the sense that the non-homogeneous patterns result from linear instability of the constant equilibrium. In comparison, a large repulsive memory-based movement can produce time-periodic patterns that do not exist for the Turing mechanism in the strong kernel case. The results above also reveal the subtle difference of the weak and strong kernels on the pattern formation: for both weak and strong kernels, a strong attractive memory-based movement (i.e., $d_2 > 0$ and $|d_2|$ is large) induces spatial patterns; but only for the strong kernel, a strong repulsive memory-based movement (i.e., $d_2 < 0$ and $|d_2|$ is large) can induce spatiotemporal patterns through Hopf bifurcations. It should be noted that the weak kernel case (Keller–Segel chemotaxis model with growth) has been studied extensively in recent years (Kuto et al. 2012; Ma and Wang 2015; Mimura and Tsujikawa 1996; Painter and Hillen 2011; Tello and Winkler 2007). Not only non-homogeneous steady-state solutions have been found analytically through bifurcation methods, but non-homogeneous periodic orbits and even chaotic dynamics have also been found numerically (Kuto et al. 2012; Painter and Hillen 2011). Here we rigorously show the existence of spatial and temporal doubly-periodic orbits (checkerboard patterns) for the strong kernel and repulsive case, which is also interesting for the chemotaxis model as repulsive chemotaxis is usually thought to be a stabilizing force (Tao 2013; Wang and Zhao 2013). Spatially non-homogeneous time-periodic orbits for chemotaxis models were also found in (Liu et al. 2013) for an attractive-repulsive Keller–Segel model and in (Zuo and Song xxx) for a predator-prey system with indirect prey-taxis.

This paper is organized as follows. We derive the equivalent systems of Eq. (1.1) for the weak and strong kernel cases, respectively in Sect. 2. In Sect. 3, for the weak kernel case, we study the stability of the constant equilibrium of the equivalent system and provide a detailed bifurcation analysis and give the conditions for pattern formation. The bifurcation analysis of the strong kernel case is given in Sect. 4. We apply our general results to a logistic growth model in Sect. 5, and the bifurcation direction and

stability of the steady-state are determined. Finally, we conclude and discuss our work in Sect. 6, and some detailed proofs and calculations are given in the "Appendix".

In the paper the space of measurable functions for which the $p$-th power of the absolute value is Lebesgue integrable defined on a bounded and smooth domain $\Omega \subseteq \mathbb{R}^m$ is denoted by $L^p(\Omega)$ and we use $W^{k,p}(\Omega)$ to denote the real-valued Sobolev space based on $L^p(\Omega)$ space. Denote $X = \{u \in W^{2,p}(\Omega) : \partial_n u = 0, \ x \in \partial\Omega\}$ and $Y = L^p(\Omega)$, where $p > m$. We denote by $\mathbb{N}$ the set of all the positive integers, and $\mathbb{N}_0 = \mathbb{N} \cup \{0\}$.

## 2 Equivalence of systems

In this section, we establish the equivalence between the scalar Eq. (1.1) and chemotactic-diffusive systems without nonlocal delay. By a similar method in Theorems 2.3 and 2.4 in (Zuo and Shi 2021), we have the following results on the equivalence of the two systems under weak or strong kernel.

**Lemma 1** *Suppose that kernel $g(t)$ is given by the weak kernel function $g_w(t) = \frac{1}{\tau}e^{-\frac{t}{\tau}}$, and define*

$$v(x,t) = (g_w * G * u)(x,t) = \int_{-\infty}^{t} \int_{\Omega} G(x,y,t-s)g_w(t-s)u(y,s)dyds. \quad (2.1)$$

1. *If $u(x,t)$ is the solution of (1.1) and $v(x,t)$ is defined by (2.1), that $(u(x,t), v(x,t))$ is the solution of*

$$\begin{cases} u_t(x,t) = d_1\Delta u(x,t) + d_2 div(u(x,t)\nabla v(x,t)) + f(u(x,t)), & x \in \Omega, \ t > 0, \\ v_t(x,t) = d_1\Delta v(x,t) + \frac{1}{\tau}(u(x,t) - v(x,t)), & x \in \Omega, \ t > 0, \\ \partial_n u(x,t) = \partial_n v(x,t) = 0, & x \in \partial\Omega, \ t > 0, \\ u(x,0) = \eta(x,0), & x \in \Omega, \\ v(x,0) = \frac{1}{\tau}\int_{-\infty}^{0}\int_{\Omega} G(x,y,-s)e^{\frac{s}{\tau}}\eta(y,s)dyds, & x \in \Omega. \end{cases}$$
$$(2.2)$$

2. *If $(u(x,t), v(x,t))$ is a solution of*

$$\begin{cases} u_t(x,t) = d_1\Delta u(x,t) + d_2 div(u(x,t)\nabla v(x,t)) + f(u(x,t)), & x \in \Omega, \ t \in \mathbb{R}, \\ v_t(x,t) = d_1\Delta v(x,t) + \frac{1}{\tau}(u(x,t) - v(x,t)), & x \in \Omega, \ t \in \mathbb{R}, \\ \partial_n u(x,t) = \partial_n v(x,t) = 0, & x \in \partial\Omega, \ t \in \mathbb{R}. \end{cases}$$
$$(2.3)$$

*Then $u(x,t)$ satisfies Eq. (1.1) such that $\eta(x,s) = u(x,s)$ for $-\infty < s < 0$. In particular, if $(u(x), v(x))$ is a steady state solution of (2.3), then $u(x)$ is a steady state solution of (1.1); and if $(u(x,t), v(x,t))$ is a periodic solution of (2.3), then $u(x,t)$ is a periodic solution of (1.1).*

For the strong kernel case, we can similarly obtain the following equivalence.

**Lemma 2** *Suppose that kernel $g(t)$ is given by the strong kernel function $g_s(t) = \frac{t}{\tau^2}e^{-\frac{t}{\tau}}$, and define*

$$v(x,t) = g_s * G * u(x,t) = \int_{-\infty}^{t} \int_{\Omega} G(x,y,t-s)g_s(t-s)u(y,s)dyds. \quad (2.4)$$

1. *If $u(x,t)$ is the solution of (1.1) and $v(x,t)$ is defined as in (2.4), then $(u(x,t), v(x,t), w(x,t))$ is the solution of*

$$
\begin{cases}
u_t(x,t) = d_1\Delta u(x,t) + d_2 div(u(x,t)\nabla v(x,t)) + f(u(x,t)), & x \in \Omega, \ t > 0, \\
v_t(x,t) = d_1\Delta v(x,t) + \frac{1}{\tau}(w(x,t) - v(x,t)), & x \in \Omega, \ t > 0, \\
w_t(x,t) = d_1\Delta w(x,t) + \frac{1}{\tau}(u(x,t) - w(x,t)), & x \in \Omega, \ t > 0, \\
\partial_n u(x,t) = \partial_n v(x,t) = \partial_n w(x,t) = 0, & x \in \partial\Omega, \ t > 0, \\
u(x,0) = \eta(x,0), & x \in \Omega, \\
v(x,0) = \int_{-\infty}^{0} \int_{\Omega} G(x,y,-s)\frac{-s}{\tau^2}e^{\frac{s}{\tau}}\eta(y,s)dyds, & x \in \Omega, \\
w(x,0) = \int_{-\infty}^{0} \int_{\Omega} G(x,y,-s)\frac{1}{\tau}e^{\frac{s}{\tau}}\eta(y,s)dyds, & x \in \Omega.
\end{cases}
$$
$$(2.5)$$

2. *If $(u(x,t), v(x,t), w(x,t))$ is a solution of*

$$
\begin{cases}
u_t(x,t) = d_1\Delta u(x,t) + d_2 div(u(x,t)\nabla v(x,t)) + f(u(x,t)), & x \in \Omega, \ t \in \mathbb{R}, \\
v_t(x,t) = d_1\Delta v(x,t) + \frac{1}{\tau}(w(x,t) - v(x,t)), & x \in \Omega, \ t \in \mathbb{R}, \\
w_t(x,t) = d_1\Delta w(x,t) + \frac{1}{\tau}(u(x,t) - w(x,t)), & x \in \Omega, \ t \in \mathbb{R}, \\
\partial_n u(x,t) = \partial_n v(x,t) = \partial_n v(x,t) = 0, & x \in \partial\Omega, \ t \in \mathbb{R}.
\end{cases}
$$
$$(2.6)$$

*Then $u(x,t)$ satisfies Eq. (1.1) with the strong kernel $g_s(t)$ such that $\eta(x,s) = u(x,s)$ for $-\infty < s < 0$. In particular, if $(u(x), v(x), w(x))$ is a steady state solution of (2.6), then $u(x)$ is a steady state solution of (1.1); if $(u(x,t), v(x,t), w(x,t))$ is a periodic solution of (2.6), then $u(x,t)$ is a periodic solution of (1.1).*

From Lemmas 1 and 2, one can see the existence of steady states and periodic solutions of Eq. (1.1) with Gamma temporal distribution function and diffusion spatiotemporal kernel function. Next we show the equivalence of the stability of the constant equilibrium with respect to the two systems. From the assumption (H1), Eq. (1.1) has a positive constant equilibrium $u = \theta$. The linearization of Eq. (1.1) at $u = \theta$ is

$$
\begin{cases}
\psi_t(x,t) = d_1\Delta\psi(x,t) + d_2\theta\Delta\left(\int_{\Omega}\int_{-\infty}^{t} G(x,y,t-s)g(t-s)\psi(y,s)dyds\right) \\
\qquad + f'(\theta)\psi, & x \in \Omega, \ t > 0, \quad (2.7) \\
\partial_n\psi(x,t) = 0, & x \in \partial\Omega, \ t > 0.
\end{cases}
$$

By assuming that $\psi(x, t) = e^{\mu t}\varphi(x)$, the eigenvalue problem of Eq. (2.7) is given by

$$\mu\varphi = d_1\Delta\varphi + d_2\theta\Delta\left(\int_\Omega\int_{-\infty}^t G(x, y, t-s)g(t-s)e^{\mu s}\varphi(y)dyds\right) + f'(\theta)\varphi, \tag{2.8}$$

where $\mu \in \mathbb{C}$ and $\varphi \in X\backslash\{0\}$.

**Lemma 3** *$\mu \in \mathbb{C}$ is an eigenvalue of Eq. (2.8) if and only if there exist some $n \in \mathbb{N}_0$ such that $\mu$ is a root of the following equation:*

$$\mu + d_1\lambda_n + \frac{d_2\theta\lambda_n}{(1 + d_1\lambda_n\tau + \mu\tau)^{m+1}} - f'(\theta) = 0, \tag{2.9}$$

*where $\lambda_n$ and $\phi_n$ are the eigenvalues and the corresponding eigenfunctions of (1.4), and $m = 0$ for the weak kernel and $m = 1$ for the strong kernel.*

**Proof** We take the weak kernel as an example to demonstrate the calculation. First, we substitute (1.3), (1.6) and $\varphi(x) = \phi_n(x)$ into Eq. (2.8) and obtain

$$
\begin{aligned}
\mu\phi_n(x)e^{\mu t} &= -d_1\lambda_n\phi_n(x)e^{\mu t} + \frac{d_2\theta}{\tau}\left(\int_\Omega\int_{-\infty}^t\sum_{n=1}^\infty e^{-d_1\lambda_n(t-s)}\phi_n(x)\phi_n^2(y)e^{-(t-s)/\tau}e^{\mu s}dyds\right) \\
&\quad - f'(\theta)\phi_n(x)e^{\mu t} \\
&= -d_1\lambda_n\phi_n(x)e^{\mu t} + \frac{d_2\theta}{\tau}\int_{-\infty}^0 e^{(d_1\lambda_n+1/\tau)s}e^{\mu s}ds\int_\Omega\phi_n^2(y)dy\phi_n(x)e^{\mu t} \\
&\quad - f'(\theta)\phi_n(x)e^{\mu t} \\
&= -d_1\lambda_n\phi_n(x)e^{\mu t} + \frac{d_2\theta}{1+d_1\lambda_n\tau+\mu\tau}\phi_n(x)e^{\mu t} - f'(\theta)\phi_n(x)e^{\mu t}.
\end{aligned}
$$

Eliminating $\phi_n(x)e^{\mu t}$ from both sides, we obtain the characteristic Eq. (2.9) when $m = 0$ for the weak kernel case. The calculation for the strong kernel case is similar. $\square$

**Theorem 1** *For Eq. (1.1) with the spatial kernel $G$ taken as (1.3) and temporal kernel $g$ taken as (1.6), the constant equilibrium $u = \theta$ is locally asymptotically stable (unstable) when the equilibrium of the equivalent system (2.3) or (2.6) is locally asymptotically stable (unstable).*

**Proof** Here we still demonstrate the weak kernel case. From Lemma 3, the eigenvalues of the linear equation of Eq. (1.1) with weak kernel satisfy

$$\mu + d_1\lambda_n + \frac{d_2\theta\lambda_n}{1 + d_1\lambda_n\tau + \mu\tau} - f'(\theta) = 0. \tag{2.10}$$

By the method of separation of variables for classical linear reaction–diffusion equations, it is easy to obtain the characteristic equation for its equivalent two-component system (2.2):

$$(\mu + d_1\lambda_n - f'(\theta))\left(\mu + d_1\lambda_n + \frac{1}{\tau}\right) + \frac{d_2\theta\lambda_n}{\tau} = 0. \tag{2.11}$$

A direct calculation shows that Eqs. (2.10) and (2.11) are completely equivalent to each other. A similar procedure can be applied to the strong kernel case, and even Gamma functions with a larger $m$.

**Remark 1**  1. Eq. (1.1) with the spatial kernel $G$ taken as (1.3) and temporal kernel $g$ as the general Gamma distribution function of order $n$ in (1.5) is equivalent to a system of $(n + 1)$ reaction–diffusion equations, and the system consists of one equation with chemotaxis and $n$ linear equations.
2. The equivalence of stability in Lemma 3 and Theorem 1 also hold for general Gamma distribution function of order $n$, and the characteristic equation is (2.9) for $m = n$.

## 3 Weak kernel case

From Theorem 1, the stability of the constant equilibrium $u = \theta$ with respect to (1.1) for the weak kernel case can be equivalently obtained through analyzing the following reaction–diffusion-taxis system:

$$\begin{cases} u_t(x, t) = d_1 \Delta u(x, t) + d_2 div(u(x, t)\nabla v(x, t)) + f(u(x, t)), & x \in \Omega, \ t > 0, \\ v_t(x, t) = d_1 \Delta v(x, t) + \frac{1}{\tau}(u(x, t) - v(x, t)), & x \in \Omega, \ t > 0, \\ \partial_n u(x, t) = \partial_n v(x, t) = 0, & x \in \partial\Omega, \ t > 0, \end{cases}$$
(3.1)

which admits a constant equilibrium $(\theta, \theta)$. Here we analyze the stability of $(\theta, \theta)$ with respect to (3.1) and associated bifurcations of non-constant steady states. Similar stability analysis and bifurcation results have also been obtained in, for example, (Painter and Hillen 2011; Ma and Wang 2015). We will provide a detailed calculation of the bifurcation direction and the stability of the bifurcating steady state.

First we linearize Eq. (3.1) at $(\theta, \theta)$, and the stability of $(\theta, \theta)$ with respect to (3.1) is determined by the following eigenvalue problem

$$\begin{cases} d_1 \Delta\varphi + d_2\theta\Delta\psi + f'(\theta)\varphi = \mu\varphi, & x \in \Omega, \\ d_1 \Delta\psi + \frac{1}{\tau}(\varphi - \psi) = \mu\psi, & x \in \Omega, \\ \partial_n\varphi = \partial_n\psi = 0, & x \in \partial\Omega. \end{cases}$$
(3.2)

By using the results of Lemma 3.1 in Shi et al. (2020), the eigenvalues of (3.2) are the eigenvalues of Jacobian matrix

$$J_n^w = \begin{pmatrix} -d_1\lambda_n + f'(\theta) & -d_2\theta\lambda_n \\ \frac{1}{\tau} & -d_1\lambda_n - \frac{1}{\tau} \end{pmatrix},$$
(3.3)

where $\lambda_n$ are the eigenvalues of (1.4) for $n \in \mathbb{N}_0$. Hence we have the characteristic equations:

$$\mu^2 + T_n\mu + D_n = 0, \quad n \in \mathbb{N}_0,$$
(3.4)

with

$$T_n = 2d_1\lambda_n + \frac{1}{\tau} - f'(\theta), \quad D_n = d_1^2\lambda_n^2 + \left(\frac{d_1 + d_2\theta}{\tau} - d_1 f'(\theta)\right)\lambda_n - \frac{f'(\theta)}{\tau}. \quad (3.5)$$

Note that $T_n = Trace(J_n^w)$ and $D_n = Det(J_n^w)$.

From (H1) we have $f'(\theta) < 0$, hence $T_n > 0$ holds for all $n \in \mathbb{N}_0$. However, the necessary condition for a Hopf bifurcation which is $T_n = 0$ cannot be satisfied. If instead we have $f'(\theta) > 1/\tau > 0$, Hopf bifurcations are possible but the bifurcating periodic solutions are unstable as the equilibrium $u = \theta$ is unstable. For steady-state bifurcations we have the following results for Eq. (3.4).

**Lemma 4** *For $n \in \mathbb{N}$, define*

$$d_{2,n}^w = \frac{(f'(\theta) - d_1\lambda_n)(d_1\lambda_n\tau + 1)}{\theta\lambda_n}, \quad d_2^* = \max_{n \in \mathbb{N}} d_{2,n}^w \quad (3.6)$$

*Then the following results hold:*

(i) *Eq. (3.4) has no purely imaginary roots for any $d_2 \in \mathbb{R}$;*
(ii) *$\mu = 0$ is a root of Eq. (3.4) if and only if $d_2 = d_{2,n}^w$;*
(iii) *when $d_2 > d_2^*$, all the eigenvalues of Eq. (3.4) have negative real parts; and when $d_2 < d_2^*$, (3.4) has at least one eigenvalue with positive real part.*

**Proof** Since $f'(\theta) < 0$, $\lambda_n > 0$ and $\lim_{n\to\infty} \lambda_n = \infty$, we have $d_{2,n}^w < 0$ for $n \in \mathbb{N}$ and $\lim_{n\to\infty} d_{2,n}^w = -\infty$. Hence $d_2^* = \max_{n \in \mathbb{N}} d_{2,n}^w = \sup_{n \in \mathbb{N}} d_{2,n}^w < 0$ exists.

The conclusion (i) can be easily seen as $T_n > 0$ for all $n \in \mathbb{N} \cup \{0\}$ and any $d_2 \in \mathbb{R}$, while $T_n = 0$ is the necessary condition for Eq. (3.4) to have purely imaginary roots. Taking $d_2$ as the bifurcation parameter, we immediately obtain the steady-state bifurcation points $d_2 = d_{2,n}^w$ satisfying $D_n(d_{2,n}^w) = 0$ such that Eq. (3.4) has a zero eigenvalue. This proves (ii). Part (iii) is a direct consequence of the definition of $d_2^*$.

Based on Lemma 4, we obtain the following results for the stability of $(\theta, \theta)$ of Eq. (3.1).

**Theorem 2** *Suppose that $d_1$, $d_2$, $f$ satisfy (H1) and (H2), and let $d_2^*$ be defined in Lemma 4. Then, $(\theta, \theta)$ is locally asymptotically stable if $d_2 \geq d_2^*$ and it is unstable if $d_2 < d_2^*$.*

Next, we show the bifurcation of the non-constant steady-state solutions following (Crandall and Rabinowitz 1971; Shi 1999; Shi and Wang 2009). A steady state of Eq. (3.1) is a solution of the elliptic system:

$$\begin{cases} d_1\Delta u + d_2 div(u\nabla v) + f(u) = 0, & x \in \Omega, \\ d_1\Delta v + \frac{1}{\tau}(u - v) = 0, & x \in \Omega, \\ \partial_n u = \partial_n v = 0, & x \in \partial\Omega. \end{cases} \quad (3.7)$$

In the following, we prove the occurrence of steady-state bifurcations in system (3.7).

**Theorem 3** *Suppose that $d_1$, $d_2$ and $f$ satisfy (H1) and (H2), and let $d_2^*$, $d_{2,n}^w$ be defined in Lemma 4.*

(i) *Suppose that $\lambda_n$ is a simple eigenvalue of (1.4), and $d_{2,n}^w \neq d_{2,k}^w$ for any $k \in \mathbb{N}$ and $k \neq n$. Then $d_2 = d_{2,n}^w$ is a bifurcation point for (3.7). More precisely, near $(d_{2,n}^w, \theta, \theta)$, there is a smooth curve $\Gamma_n$ of positive solutions of (3.7) bifurcating from the line of constant solutions $\{(d_2, \theta, \theta) : d_2 > 0\}$ with the following form:*

$$\Gamma_n = \{(d_{2,n}(s), U_n(s, x), V_n(s, x)) : -\delta < s < \delta\}, \tag{3.8}$$

*where $\delta$ is a positive constant and*

$$U_n(s, x) = \theta + s\phi_n(x) + sz_{1,n}(s, x), \quad V_n(s, x) = \theta + s\frac{\phi_n(x)}{d_1\lambda_n\tau + 1} + sz_{2,n}(s, x),$$

*with smooth functions $d_{2,n}(s)$, $z_{1,n}(s, \cdot)$, $z_{2,n}(s, \cdot)$ satisfying $d_{2,n}(0) = d_{2,n}^w$ and $z_{1,n}(0, \cdot) = 0$, $z_{2,n}(0, \cdot) = 0$;*

(ii) *If in addition, $\Omega$ is one-dimensional and $\Omega = (0, l\pi)$, then $d'_{2,n}(0) = 0$ and*

$$d''_{2,n}(0) = \frac{f'''(\theta)}{4\theta\lambda_n h_n} + \frac{2(f''(\theta) - d_{2,n}^w\lambda_n h_n)\Theta_1^0 + f''(\theta)\Theta_1^2 - 2d_{2,n}^w\lambda_n\Theta_2^2 + d_{2,n}^w\lambda_n h_n\Theta_1^2}{2\theta\lambda_n h_n}, \tag{3.9}$$

*where $\Theta_1^0$, $\Theta_1^2$, $\Theta_2^2$ are given by*

$$\Theta_1^0 = -\frac{f''(\theta)}{2f'(\theta)}, \quad \Theta_1^2 = \frac{(4d_{2,n}^w\lambda_n h_n - f''(\theta))(1 + 4d_1\lambda_n\tau)}{2[(f'(\theta) - 4d_1\lambda_n)(1 + 4d_1\tau\lambda_n)^2 - 4d_{2,n}^w\theta\lambda_n]},$$

$$\Theta_2^2 = \frac{4d_{2,n}^w\lambda_n h_n - f''(\theta)}{2[(f'(\theta) - 4d_1\lambda_n)(1 + 4d_1\tau\lambda_n)^2 - 4d_{2,n}^w\theta\lambda_n]}, \tag{3.10}$$

*and $\lambda_n = n^2/l^2$, $h_n = 1/(1 + d_1\lambda_n\tau)$. Let $d_{2,N}^w = d_2^*$. If $d''_{2,N}(0) < 0$, the bifurcation at $d_2 = d_2^* = d_{2,N}^w$ is supercritical and the bifurcating steady states are locally asymptotically stable; if $d''_{2,N}(0) > 0$, the bifurcation at $d_2 = d_2^* = d_{2,N}^w$ is subcritical and the bifurcating steady states are unstable; all other bifurcating steady states from $d_{2,n}^w$ with $n \neq N$ are unstable.*

The proof of Theorem 3 is given in the Appendix. From Theorems 2 and 3, $d_2 = d_2^* < 0$ is a critical diffusion rate where the constant steady state $(\theta, \theta)$ changes stability, and it is rigorously shown that small amplitude stable non-homogeneous steady state solutions could bifurcate from the constant ones at $d_2 = d_2^*$.

*Remark 2*  1. Theorem 3 is a local bifurcation result as the nonlinear function $f$ is only defined in a neighborhood of $u = \theta$. One may obtain a global bifurcation diagram by the abstract bifurcation theorem in (Shi and Wang 2009) for a globally defined nonlinearity $f(u)$, but this is not pursued here.
2. In the discrete delay model considered in (Shi et al. 2020), a necessary condition for pattern formation is that $|d_2| > d_1/\theta$. In the case of (1.1) with weak kernel, a

necessary condition for pattern formation is $d_2 < d_2^* \le -(\sqrt{-\tau f'(\theta)} + 1)^2 d_1/\theta$ which implies that $d_2 < -d_1/\theta$. Thus, we see that $|d_2| > d_1/\theta$ is still necessary for the pattern formation in the distributed delay case, but the delay value $\tau$ increases the threshold $|d_2^*| = |d_2^*(\tau)|$. To achieve pattern formation, the magnitude of the memory-based diffusion needs to be larger in the distributed delay case than in the discrete delay case.

3. The average delay value $\tau$ also affects the pattern selection. Let $N$ be the dominant wave number which satisfies $d_{2,N}^w = d_2^*$ as in Theorem 3. Then $N$ is non-increasing with respect to $\tau$. Indeed one can observe that when we consider $d_{2,n}^w$ as a function of continuous variable $p = \lambda_n$ in (3.6), it reaches it maximum at $p = \sqrt{\frac{-f'(\theta)}{\tau d_1^2}}$. Hence

$$\lambda_N = \frac{N^2}{l^2} \approx \sqrt{\frac{-f'(\theta)}{\tau d_1^2}}, \tag{3.11}$$

which implies that $N$ is non-increasing with respect to $\tau$.

## 4 Strong kernel case

From Theorem 1, the stability of the constant equilibrium $u = \theta$ with respect to (1.1) for the strong kernel case can be equivalently obtained through analyzing the following reaction–diffusion system with chemotaxis:

$$\begin{cases} u_t(x, t) = d_1 \Delta u(x, t) + d_2 div(u(x, t)\nabla v(x, t)) + f(u(x, t)), & x \in \Omega, \ t > 0, \\ v_t(x, t) = d_1 \Delta v(x, t) + \frac{1}{\tau}(w(x, t) - v(x, t)), & x \in \Omega, \ t > 0, \\ w_t(x, t) = d_1 \Delta w(x, t) + \frac{1}{\tau}(u(x, t) - w(x, t)), & x \in \Omega, \ t > 0, \\ \partial_n u(x, t) = \partial_n v(x, t) = \partial_n w(x, t) = 0, & x \in \partial\Omega, \ t > 0, \end{cases} \tag{4.1}$$

which admits a constant equilibrium $(\theta, \theta, \theta)$. Linearizing Eq. (4.1) at $(\theta, \theta, \theta)$, the stability of $(\theta, \theta, \theta)$ is determined by the following eigenvalue problem:

$$\begin{cases} d_1 \Delta\phi + d_2\theta\Delta\psi + f'(\theta)\phi = \mu\phi, & x \in \Omega, \\ d_1 \Delta\psi + \frac{1}{\tau}(\varphi - \psi) = \mu\psi, & x \in \Omega, \\ d_1 \Delta\varphi + \frac{1}{\tau}(\phi - \varphi), & x \in \Omega, \\ \partial_n\phi = \partial_n\psi = \partial_n\varphi, & x \in \partial\Omega. \end{cases} \tag{4.2}$$

Similar to the weak kernel case, the eigenvalues of (4.2) are the eigenvalues of the Jacobian matrix

$$J_n^s = \begin{pmatrix} -d_1\lambda_n + f'(\theta) & -d_2\theta\lambda_n & 0 \\ 0 & -d_1\lambda_n - \frac{1}{\tau} & \frac{1}{\tau} \\ \frac{1}{\tau} & 0 & -d_1\lambda_n - \frac{1}{\tau} \end{pmatrix},$$

where $\lambda_n$ is the eigenvalues of (1.4) for $n \in \mathbb{N}_0$. Hence we have the characteristic equations

$$\mu^3 + A_n \mu^2 + B_n \mu + C_n = 0, \quad n \in \mathbb{N}_0, \tag{4.3}$$

with

$$A_n = 3d_1 \lambda_n + \frac{2}{\tau} - f'(\theta),$$

$$B_n = \left(d_1 \lambda_n + \frac{1}{\tau}\right)^2 + 2(d_1 \lambda_n - f'(\theta))\left(d_1 \lambda_n + \frac{1}{\tau}\right),$$

$$C_n = d_1^3 \lambda_n^3 + \left(\frac{2d_1^2}{\tau} - f'(\theta)d_1^2\right)\lambda_n^2 + \left(\frac{d_1 + d_2\theta}{\tau} - \frac{2f'(\theta)d_1}{\tau}\right)\lambda_n - \frac{f'(\theta)}{\tau^2}.$$
$$\tag{4.4}$$

Note that $A_n = -Trace(J_n^s)$ and $C_n = -Det(J_n^s)$. By the Routh-Hurwitz stability criterion, the matrix $J_n^s$ is stable (all eigenvalues have negative real parts) if and only if

$$A_n > 0, \quad C_n > 0, \quad A_n B_n - C_n > 0. \tag{4.5}$$

From (H1), the condition $A_n > 0$ always holds. Hence the matrix $J_n^s$ may lose the stability either via $C_n = 0$ (which implies a zero eigenvalue of $J_n^s$) or via $A_n B_n - C_n = 0$ (which implies a pair of purely imaginary eigenvalues $\pm\sqrt{B_n}i$ of $J_n^s$). Also we can observe that $B_n > 0$ always holds so $C_n = 0$ and $A_n B_n - C_n = 0$ cannot occur in the same time.

To study these two kinds of instability, we define continuous functions $A(p)$, $B(p)$, $C(p)$ for $p \in [0, \infty)$ so that $A(\lambda_n) = A_n$, $B(\lambda_n) = B_n$ and $C(\lambda_n) = C_n$. Then

$$C(p) := d_1^3 p^3 + a_1 p^2 + b_1 p + c_1,$$
$$Q(p) := A(p)B(p) - C(p) = 8d_1^3 p^3 + a_2 p^2 + b_2 p + c_2, \tag{4.6}$$

where

$$a_1 = \frac{2d_1^2}{\tau} - f'(\theta)d_1^2, \ b_1 = \frac{d_1 + d_2\theta}{\tau^2} - \frac{2f'(\theta)d_1}{\tau}, \ c_1 = -\frac{f'(\theta)}{\tau^2},$$

$$a_2 = \frac{16d_1^2}{\tau} - 8f'(\theta)d_1^2, \ b_2 = \frac{10d_1 - d_2\theta}{\tau^2} - \frac{12d_1 f'(\theta)}{\tau} + 2d_1(f'(\theta))^2,$$

$$c_2 = \frac{2}{\tau}\left(\frac{1}{\tau} - f'(\theta)\right)^2.$$

Taking $d_2$ as the bifurcation parameter, we obtain the steady-state bifurcation points:

$$d_{2,n}^S := d_2^S(\lambda_n), \ \text{with } d_2^S(p) = \frac{(f'(\theta) - d_1 p)(d_1 p\tau + 1)^2}{\theta p}, \tag{4.7}$$

and Hopf bifurcation points:

$$d_{2,n}^H := d_2^H(\lambda_n), \text{ with } d_2^H(p) = \frac{2(d_1\tau p + 1)(2d_1\tau p - f'(\theta)\tau + 1)^2}{\theta\tau p}. \tag{4.8}$$

Note that $d_2 = d_2^S(p)$ is solved from setting $C(p) = 0$, so $d_{2,n}^S$ satisfies $C(\lambda_n) = 0$. Similarly $d_2 = d_{2,n}^H$ is solved from setting $Q(p) = 0$, so $d_{2,n}^H$ satisfies $Q(\lambda_n) = 0$.

Some basic properties of functions $d_2^S(p)$ and $d_2^H(p)$ are stated in the following lemma.

**Lemma 5** *For $d_2^S(p)$ and $d_2^H(p)$ defined in* (4.7) *and* (4.8)*, we have*

(i) *there exists $p_* > 0$ such that $d_2^S(p)$ is increasing for $p \in (0, p_*)$ and decreasing for $p \in (p_*, +\infty)$, and $d_2^S(p)$ attains its global maximum value $d_{2,S}^* < 0$ at $p = p_*$. Moreover, we have $\lim_{p\to 0} d_2^S(p) = -\infty$ and $\lim_{p\to +\infty} d_2^S(p) = -\infty$.*

(ii) *there exists $p^* > 0$ such that $d_2^H$ is decreasing for $p \in (0, p^*)$ and increasing for $p \in (p^*, +\infty)$, and $d_2^H(p)$ attains its global minimum value $d_{2,H}^* > 0$ at $p = p^*$. Moreover, we have $\lim_{p\to 0} d_2^H(p) = +\infty$ and $\lim_{p\to +\infty} d_2^H(p) = +\infty$.*

**Proof** With the expression of $d_2^S(p)$ given in (4.7), we calculate the derivative of $d_2^S(p)$ with respect to $p$ and obtain

$$\frac{d}{dp}d_2^S(p) = \frac{(d_1 p\tau + 1)H(p)}{\theta^2 p^2}, \tag{4.9}$$

with

$$H(p) = -2d_1^2\tau\theta p^2 + d_1\tau\theta f'(\theta)p - f'(\theta)\theta.$$

From Eq. (4.9), we can see that the sign of the derivative of $d_2^S(p)$ is the same as the one of $H(p)$ which is a quadratic function with a unique positive root $p_*$. Thus, we have $H(p) > 0$ for $p \in (0, p_*)$ and $H(p) < 0$ for $p \in (p_*, +\infty)$. The limits of $d_2^S$ when $p \to 0$ and $p \to +\infty$ can be attained through a direct calculation. This proves part (i). Part (ii) can be proved in a similar way. $\quad\blacksquare$

We obtain the stability of $(\theta, \theta, \theta)$ for Eq. (4.1) as follows.

**Proposition 1** *Suppose that $d_1$, $d_2$, $f$ satisfy conditions (H1) and (H2) and $\tau > 0$. Define*

$$d_{2,S}^* := \max_{n\in\mathbb{N}} \left\{d_{2,n}^S\right\}, \quad d_{2,H}^* := \min_{n\in\mathbb{N}} \left\{d_{2,n}^H\right\}, \tag{4.10}$$

*where $d_{2,n}^S$ and $d_{2,n}^H$ are defined in* (4.7) *and* (4.8)*.*

(i) *when $d_{2,S}^* < d_2 < d_{2,H}^*$, all the eigenvalues of Eq. (4.3) have negative real parts, and $(\theta, \theta, \theta)$ is locally asymptotically stable with respect to* (4.1)*;*

(ii) *when $d_2 > d_{2,H}^*$, $(\theta, \theta, \theta)$ is unstable and $\mu = \pm i\omega_0$ ($\omega_0 > 0$) is a pair of purely imaginary roots of Eq. (4.3) if $d_2 = d_{2,n}^H$;*

(iii) *when* $d_2 < d_{2,S}^*$, $(\theta, \theta, \theta)$ *is unstable and* $\mu = 0$ *is a root of Eq.* (4.3) *if* $d_2 = d_{2,n}^S$.

**Proof** From Lemma 5, $\lambda_n > 0$ and $\lim\limits_{n \to \infty} \lambda_n = \infty$, $d_{2,S}^*$ and $d_{2,H}^*$ exist and $d_{2,S}^* < 0 < d_{2,H}^*$. From Lemma 5, when $d_{2,S}^* < d_2 < d_{2,H}^*$, we have $C(p) > 0$ and $Q(p) > 0$ for all $p > 0$ so all the eigenvalues of $J_n^s$ have negative real parts for $n \in \mathbb{N}_0$ thus $(\theta, \theta, \theta)$ is locally asymptotically stable. When $d_2 < d_{2,n}^S$, we have $C_n < 0$ so the matrix $J_n^s$ has at least one eigenvalue with positive real part, and when $d_2 = d_{2,n}^S$, $J_n^s$ has a zero eigenvalue. This implies $(\theta, \theta, \theta)$ when $d_2 < d_{2,S}^*$. When $d_2 > d_{2,n}^H$, we have $A_n > 0$, $C_n > 0$ but $A_n B_n - C_n < 0$, so the matrix $J_n^s$ is unstable, and when $d_2 = d_{2,n}^H$, $J_n^s$ has a pair of complex eigenvalues with zero real part.

From Proposition 1, Eq. (4.3) has a pair of purely imaginary eigenvalues $\pm i\omega_0$ ($\omega_0 > 0$) when $d_2 = d_{2,n}^H$. We show that the eigenvalue transversality condition holds at $d_2 = d_{2,n}^H$.

**Lemma 6** *Let* $d_{2,n}^H$ *be defined in* (4.8). *Then, Eq.* (4.3) *has a pair of roots in the form of* $\mu = \alpha(d_2) \pm i\omega(d_2)$ *when* $d_2$ *is near* $d_{2,n}^H$ *such that* $\alpha\left(d_{2,n}^H\right) = 0$ *and* $\alpha'\left(d_{2,n}^H\right) > 0$.

**Proof** We only need to show that $\alpha'\left(d_{2,n}^H\right) < 0$. Take derivative of both sides of Eq. (4.3) with respect to $d_2$ (we denote $d_2$ temporarily by $\beta$ to avoid the confusion in notation), we have

$$3\mu^2 \frac{d\mu}{d\beta} + \frac{dA_n}{d\beta}\mu^2 + 2A_n\mu\frac{d\mu}{d\beta} + \frac{dB_n}{d\beta}\mu + B_n\frac{d\mu}{d\beta} + \frac{dC_n}{d\beta} = 0. \qquad (4.11)$$

From the expressions of $A_n$, $B_n$, $C_n$ in Eq. (4.3), it is straightforward to see that

$$\frac{dA_n}{d\beta} = 0, \quad \frac{dB_n}{d\beta} = 0, \quad \frac{dC_n}{d\beta} = \frac{\theta\lambda_n}{\tau}. \qquad (4.12)$$

Substituting (4.12), $\mu = i\omega_0$, $B_n = \omega_0^2$ and $\beta = d_{2,n}^H$ into Eq. (4.11), we obtain

$$\frac{d\mu}{d\beta}\bigg|_{\beta = d_{2,n}^H} = -\frac{\theta\lambda_n}{2\tau\omega_0(-\omega_0^2 + i\omega_0 A_n)},$$

thus

$$\alpha'(d_2) = \mathcal{R}e\left(\frac{d\mu}{d\beta}\bigg|_{\beta = d_{2,n}^H}\right) = \frac{\theta\lambda_n}{2\tau(\omega_0^2 + A_n^2)} > 0.$$

Now by the Hopf bifurcation Theorem for quasilinear systems of reaction–diffusion equations (Amann 1991), Proposition 1 and Lemma 6, we obtain the following result of Hopf bifurcations in Eq. (4.1).

**Theorem 4** *Suppose that* $d_1$, $d_2$, *and* $f$ *satisfy conditions (H1) and (H2), and let* $d_{2,n}^H$ *be defined in* (4.8). *Suppose that* $\lambda_n$ *is a simple eigenvalue of* (1.4), *and* $d_{2,n}^H \neq d_{2,k}^H$

*for any $k \in \mathbb{N}$ and $k \neq n$, then a Hopf bifurcation occurs at $d_2 = d_{2,n}^H$ for Eq. (4.1) and there exist a family of periodic orbits in form of*

$$\left\{ \left( U_n(x, t, s), T_n(s), d_2^{(n)}(s) \right) : s \in (0, \delta) \right\},$$

*where $U_n(x, t, s) = (u_n(x, t, s), v_n(x, t, s), w_n(x, t, s))$ is a $T_n(s)$ periodic solution of Eq. (4.1) with $d_2 = d_2^{(n)}(s)$ satisfying*

$$d_2^{(n)}(0) = d_{2,n}^H, \quad \lim_{s \to 0} U_n(x, t, s) = (\theta, \theta, \theta), \quad \lim_{s \to 0} T_n(s) = \frac{2\pi}{\sqrt{B_n}},$$

*where $B_n$ is given in (4.4). Moreover, the bifurcating periodic orbits are spatially non-homogeneous with spatial profile $\phi_n(x)$.*

*At $d_2 = d_{2,H}^* = \min_{n \in \mathbb{N}} d_{2,n}^H$, the bifurcating periodic orbits could be locally asymptotically stable, and if $d_{2,M}^H = d_{2,H}^*$ for some $M \in \mathbb{N}$, then the stable bifurcating periodic orbits have the spatial profile $\phi_M(x)$ and are temporally oscillating with period $T_M(s)$.*

We can also prove the steady-state bifurcations for (4.1) at $d_2 = d_{2,n}^S$ similar to the weak kernel case. The steady states of (4.1) satisfy the following elliptic system:

$$\begin{cases} d_1 \Delta u(x) + d_2 div(u(x) \nabla v(x)) + f(u(x)) = 0, & x \in \Omega, \\ d_1 \Delta v(x) + \frac{1}{\tau}(w(x) - v(x)) = 0, & x \in \Omega, \\ d_1 \Delta w(x) + \frac{1}{\tau}(u(x) - w(x)) = 0, & x \in \Omega, \\ \partial_n u(x) = \partial_n v(x) = \partial_n w(x) = 0, & x \in \partial\Omega, \end{cases} \quad (4.13)$$

and $(\theta, \theta, \theta)$ is a constant solution for system (4.13). Then we have the following results.

**Theorem 5** *Suppose that $d_1$, $d_2$, and $f$ satisfy conditions (H1) and (H2), and let $d_{2,n}^S$ be defined in (4.7).*

(i) *Suppose that $\lambda_n$ is a simple eigenvalue of (1.4), and $d_{2,n}^S \neq d_{2,k}^S$ for any $k \in \mathbb{N}$ and $k \neq n$. Then $d_2 = d_{2,n}^S$ is a bifurcation point for (4.13). More precisely, near $(d_{2,n}^S, \theta, \theta, \theta)$, there is a smooth curve $\tilde{\Gamma}_n$ of positive solutions of (4.13) bifurcating from the line of constant solutions $\{(d_2, \theta, \theta, \theta) : d_2 > 0\}$ with the following form:*

$$\tilde{\Gamma}_n = \left\{ \left( \tilde{d}_{2,n}(s), U^n(s, x), V^n(s, x), W^n(s, x) \right) : -\delta < s < \delta \right\}, \quad (4.14)$$

*where*

$$U^n(s, x) = \theta + s\phi_n(x) + sg_{1,n}(s, x),$$

$$V^n(s, x) = \theta + \frac{1}{(1 + d_1\lambda_n\tau)^2} s\phi_n(x) + sg_{2,n}(s, x),$$

$$W^n(s, x) = \theta + \frac{1}{1 + d_1\lambda_n\tau} s\phi_n(x) + sg_{3,n}(s, x),$$

*and $\tilde{d}_{2,n}(s)$, $g_{i,n}(s,\cdot)(i = 1, 2, 3)$ are smooth functions defined for $s \in (0, \delta)$ such that $\tilde{d}_{2,n}(0) = d_{2,n}^S$, and $g_{i,n}(0, \cdot) = 0$ $(i = 1, 2, 3)$;*

(ii) *If in addition, $\Omega$ is one-dimensional and $\Omega = (0, l\pi)$, then $\tilde{d}'_{2,n}(0) = 0$ and*

$$\tilde{d}''_{2,n}(0) = \frac{f'''(\theta)}{4\lambda_n h_n \theta} + \frac{2(f''(\theta) - d_{2,n}^S \lambda_n h_n)\Theta_1^0) + f''(\theta)\Theta_1^2 - 2d_{2,n}^S \lambda_n \Theta_2^2 + d_{2,n}^S \lambda_n h_n \Theta_1^2}{2\theta\lambda_n h_n}, \tag{4.15}$$

*where $\Theta_1^0$, $\Theta_1^2$, $\Theta_2^2$ are given by*

$$\Theta_1^0 = -\frac{f''(\theta)}{2f'(\theta)}, \quad \Theta_1^2 = \frac{(4d_{2,n}^S \lambda_n h_n - f''(\theta))(1 + 4d_1\lambda_n\tau)}{2[(f'(\theta) - 4d_1\lambda_n)(1 + 4d_1\tau\lambda_n)^2 - 4d_{2,n}^S \theta\lambda_n]},$$

$$\Theta_2^2 = \frac{4d_{2,n}^S \lambda_n h_n - f''(\theta)}{2[(f'(\theta) - 4d_1\lambda_n)(1 + 4d_1\tau\lambda_n)^2 - 4d_{2,n}^S \theta\lambda_n]}, \tag{4.16}$$

*and $\lambda_n = n^2/l^2$, $h_n = 1/(1 + d_1\lambda_n\tau)^2$. Let $d_{2,N}^S = d_{2,S}^*$. If $\tilde{d}''_{2,N}(0) < 0$, the bifurcation at $d_2 = d_{2,S}^* = d_{2,N}^S$ is supercritical and the bifurcating steady states are locally asymptotically stable; if $\tilde{d}''_{2,N}(0) > 0$, the bifurcation at $d_2 = d_{2,S}^* = d_{2,N}^S$ is subcritical and the bifurcating steady states are unstable; all other bifurcating steady states from $d_{2,n}^S$ with $n \neq N$ are unstable.*

The proof of Theorem 5 is basically the same as the one for Theorem 3, so we omit it.

**Remark 3**   1. From Lemma 5, it is clear that all steady-state bifurcation points satisfies $d_{2,n}^S < 0$ and all Hopf bifurcation points satisfies $d_{2,n}^H > 0$ for $n \in \mathbb{N}$. These conditions implies that steady-state bifurcations only occur for negative $d_2$ (attractive chemotaxis case), and Hopf bifurcations only occur for positive $d_2$ (repulsive chemotaxis case). Thus there is no interaction between steady-state bifurcations and Hopf bifurcations in this model.

2. From (4.7), we can obtain that $d_{2,n}^S < -d_1/\theta$, thus $d_{2,S}^* < -d_1/\theta$. Similarly, we have $d_{2,H}^* > 2d_1/\theta$. Therefore, we can draw the conclusion that $|d_2| > d_1/\theta$ is still a necessary condition for pattern formation in the distributed delay case with strong kernel.

3. Again the average delay value $\tau$ affects the pattern selection for both steady-state and Hopf bifurcations. If positive integer $N$ and $M$ satisfy $d_{2,N}^S = d_{2,S}^*$ and $d_{2,M}^H = d_{2,H}^*$, then $N$ and $M$ both are non-increasing with respect to $\tau$.

## 5 An example: logistic growth

When the growth function $f(u)$ is taken as the logistic growth, Eq. (1.1) becomes

$$\begin{cases} u_t = d_1\Delta u + d_2 div(u\nabla v) + u(1-u), & x \in \Omega, \ t > 0, \\ \partial_n u = 0, & x \in \partial\Omega, \ t > 0, \end{cases} \tag{5.1}$$

where $u = u(x, t)$ and $v = v(x, t)$ is defined as (1.2). It is clear that Eq (5.1) has two constant equilibria: $u = 0$ and $u = 1$.

## 5.1 Weak kernel case

For the weak kernel case, (5.1) is equivalent to

$$\begin{cases} u_t = d_1 \Delta u + d_2 div(u \nabla v) + u(1 - u), & x \in \Omega, \ t > 0, \\ v_t = d_1 \Delta v + \frac{1}{\tau}(u - v), & x \in \Omega, \ t > 0, \\ \partial_n u = \partial_n v = 0, & x \in \partial\Omega, \ t > 0. \end{cases} \tag{5.2}$$

The trivial equilibrium $(0, 0)$ is unstable. For the positive equilibrium $(1, 1)$, we can apply Theorems 2 and 3 to obtain the stability of non-homogeneous steady states of system (5.2) as $f'(\theta) = -1$ so (H1) is satisfied. The steady-state bifurcation points are

$$d_2 = d_{2,n}^w = -\frac{(1 + d_1\lambda_n)(1 + d_1\lambda_n\tau)}{\theta\lambda_n}, \tag{5.3}$$

and for the bifurcation curves of one-dimensional domain $\Omega = (0, l\pi)$, we have $d_{2,n}'(0) = 0$ and
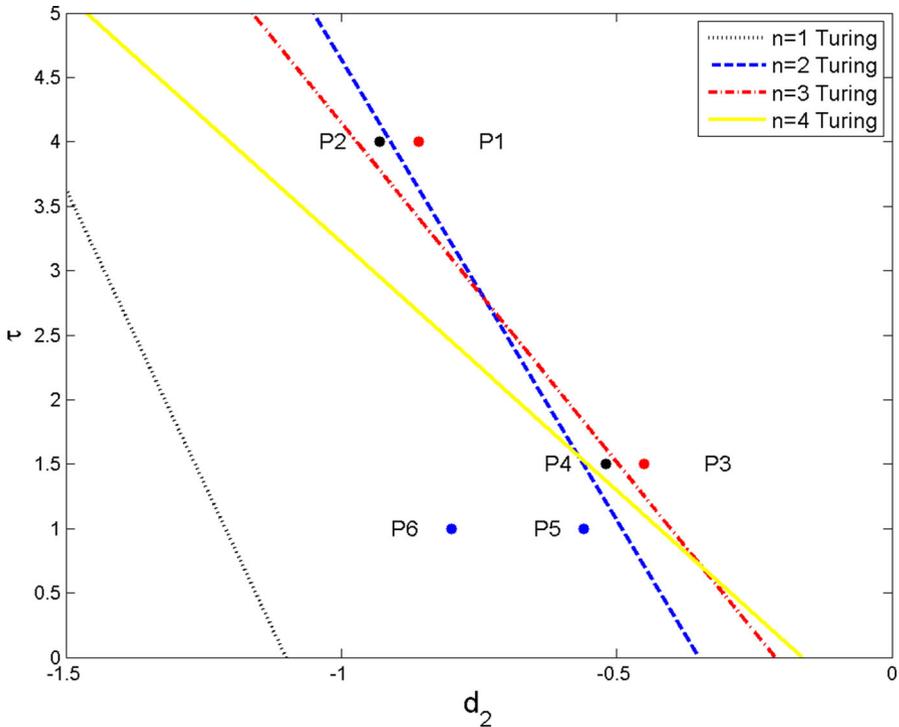
$$d_{2,n}''(0) = \frac{(1 + d_1\lambda_n\tau)(5 - 2d_1^2\lambda_n^2\tau - 5d_1\lambda_n + 28d_1^3\lambda_n^3\tau + 10d_1\lambda_n\tau - 2d_1^2\lambda_n^2)}{6\lambda_n(1 - 4d_1^2\lambda_n^2\tau)}.$$

At the dominant wave number $N$ satisfying $d_2^* = d_{2,N}^S$ where $d_2^*$ is the maximum of steady-state bifurcation points $d_{2,n}^S$, we have the approximating formula (3.11) which now becomes $d_1\lambda_N = 1/\sqrt{\tau}$. Using this yields

$$d_{2,N}''(0) = -\frac{d_1\sqrt{\tau}(1 + \sqrt{\tau})\left(10\sqrt{\tau} + \frac{23}{\sqrt{\tau}} - \frac{2}{\tau} + 3\right)}{18} < 0,$$

for any $\tau > 0$. This implies that the bifurcation direction at the dominant wave number is most likely to be supercritical and the bifurcating steady states are locally asymptotically stable.

In Fig. 1, for a fixed $\tau$, when $d_2$ varies from right to left, the constant equilibrium $(1, 1)$ loses its stability at the first Turing bifurcation curve $d_2 = d_{2,n}^w(\tau)$ as defined in (5.3). One can observe that, when $\tau$ decreases, the dominant wave number $N$ changes from $N = 2$ to $N = 3$ then $N = 4$. For example, when $\tau = 4$, the stability switch occurs at mode-2 Turing line, and the constant equilibrium is stable when $d_2 = -0.86$ (P1) and unstable when $d_2 = -0.93$ (P2) (Fig. 2 top row); when $\tau = 1.5$, the stability switch occurs at mode-3, and the constant equilibrium is stable when $d_2 = -0.45$ (P3) and unstable when $d_2 = -0.52$ (P4) (Fig. 2 middle row). In the stable case, the solution of (5.2) converges to the constant equilibrium, while in the unstable case, the solution converges to a mode-$N$ non-homogeneous steady state. When $\tau$ is chosen to be a smaller value, we also observe spatially non-homogeneous time-periodic patterns

**Fig. 1** The bifurcation diagram in parameter $(d_2, \tau)$ of system (5.2) when $d_1 = 0.1$ and $\Omega = (0, \pi)$, and the bifurcation curves $d_2 = d_{2,n}^w(\tau)$ are plotted for $n = 1, 2, 3, 4$. The points are parameter values for the numerical simulations and they are: P1 $(-0.86, 4.0)$, P2 $(-0.93, 4.0)$, P3 $(-0.45, 1.5)$, P4 $(-0.52, 1.5)$, P5 $(-0.56, 1.0)$ and P6 $(-0.8, 1.0)$
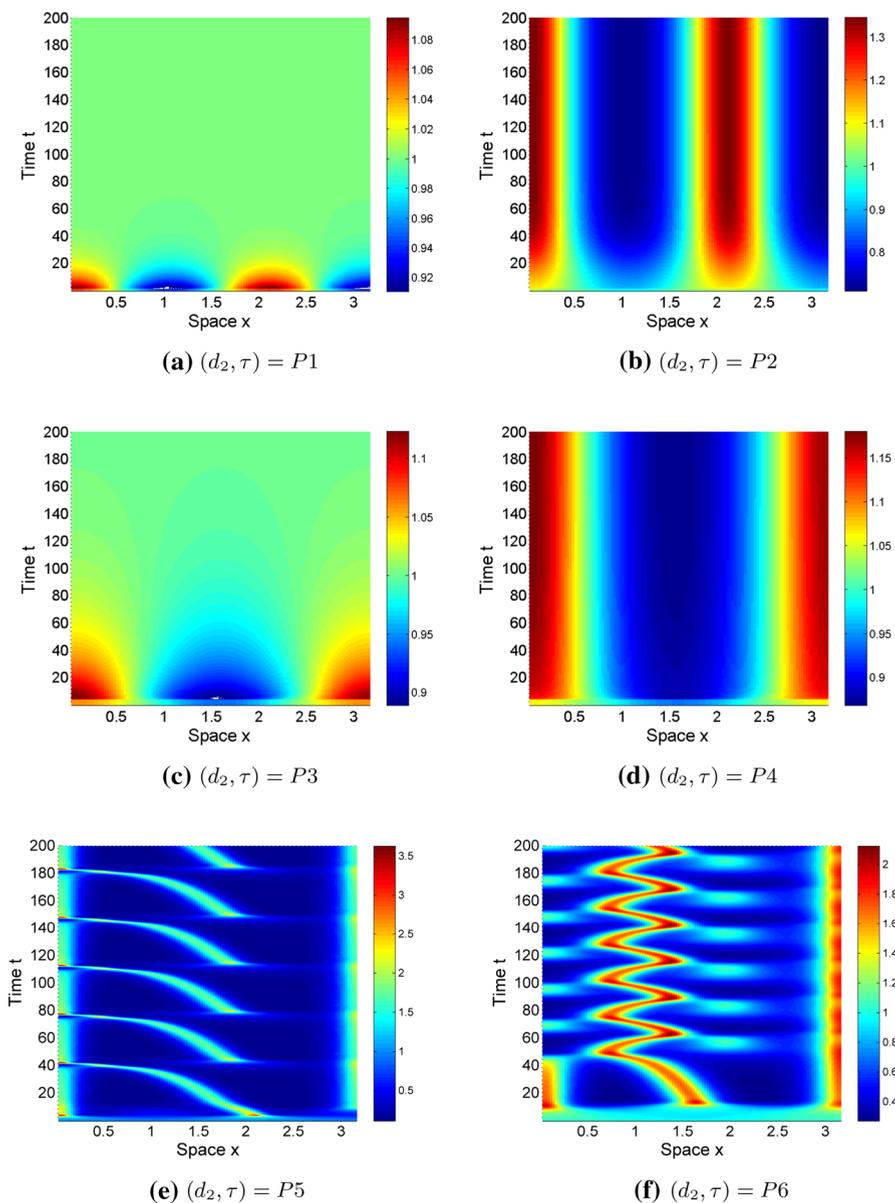
shown in Fig. 2 bottom row, which are "wandering" and "drifting" periodic patterns also observed in previous work of Keller–Segel model with growth (Painter and Hillen 2011; Ma and Wang 2015). These patterns are not a result of Hopf bifurcations from the constant equilibrium as we show that situation is impossible in Sect. 3.

## 5.2 Strong kernel case

When the distribution kernel is taken as the strong one, the equivalent system of Eq. (5.1) is

$$
\begin{cases}
u_t = d_1 \Delta u + d_2 div(u \nabla v) + u(1 - u), & x \in \Omega, \ t > 0, \\
v_t = d_1 \Delta v + \frac{1}{\tau}(w - v), & x \in \Omega, \ t > 0, \\
w_t = d_1 \Delta w + \frac{1}{\tau}(u - w), & x \in \Omega, \ t > 0, \\
\partial_n u = \partial_n v = \partial_n w = 0, & x \in \partial\Omega, \ t > 0.
\end{cases} \tag{5.4}
$$

The trivial equilibrium $(0, 0, 0)$ is unstable, we can apply Theorems 5 and 4 for the stability of the positive equilibrium $(1, 1, 1)$ and the bifurcation of non-homogeneous steady states and periodic orbits of system (5.4). The steady-state bifurcations occur
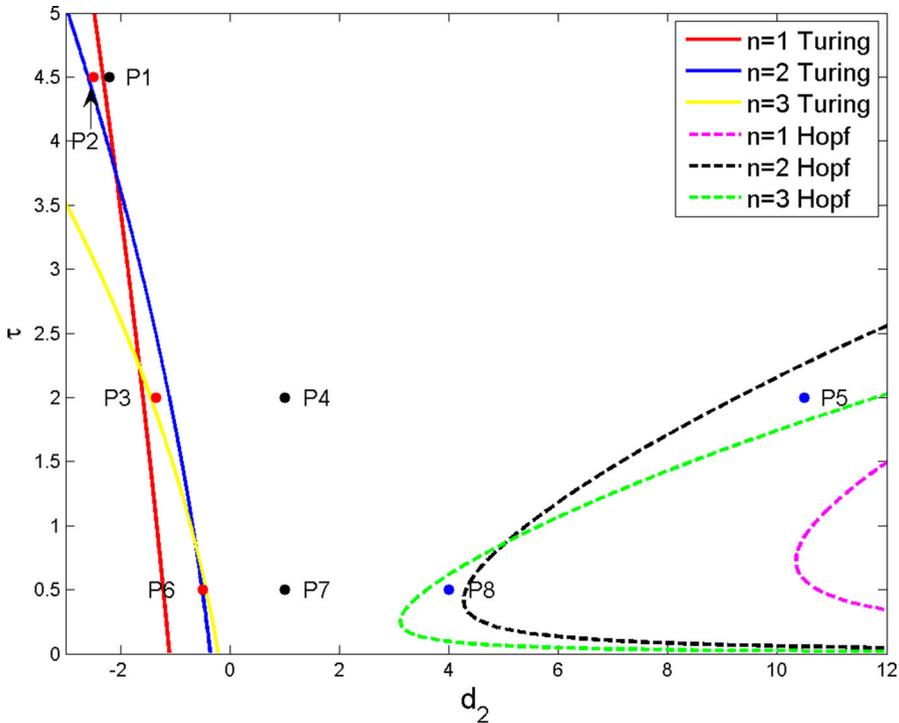
**(a)** $(d_2, \tau) = P1$

**(b)** $(d_2, \tau) = P2$

**(c)** $(d_2, \tau) = P3$

**(d)** $(d_2, \tau) = P4$

**(e)** $(d_2, \tau) = P5$

**(f)** $(d_2, \tau) = P6$

**Fig. 2** Numerical simulations of system (5.2) when parameters are $d_1 = 0.1$ and $\Omega = (0, \pi)$. In each figure, the color indicates the value of $u(x, t)$ according to colorbar

at

$$d_2 = d_{2,n}^S := -\frac{(1 + d_1\lambda_n)(1 + d_1\lambda_n\tau)^2}{\theta\lambda_n} < 0, \tag{5.5}$$
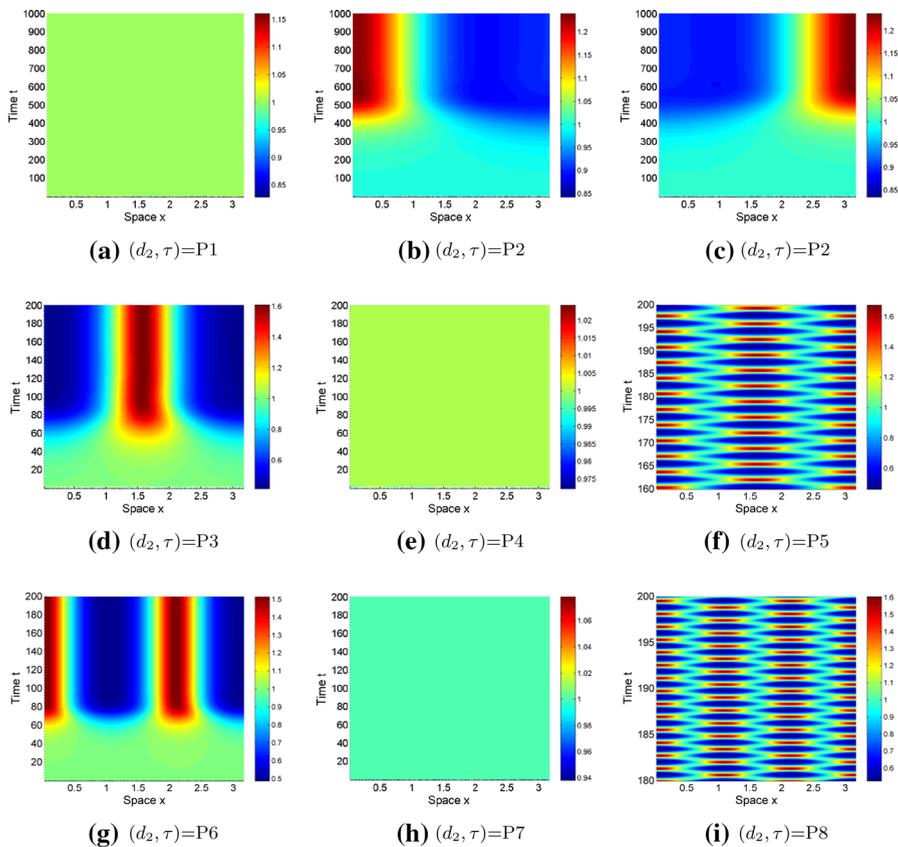
and the Hopf bifurcations occur at

**Fig. 3** The bifurcation diagram in parameter $(d_2, \tau)$ of system (5.4) when $d_1 = 0.1$ and $\Omega = (0, \pi)$, and the steady-state bifurcation curves $d_2 = d_{2,n}^S(\tau)$ (for $d_2 < 0$) and Hopf bifurcation curves $d_2 = d_{2,n}^H(\tau)$ (for $d_2 > 0$) are plotted for $n = 1, 2, 3$. The points are parameter values for the numerical simulations and they are: P1 $(-2.5, 4.5)$, P2 $(-2.2, 4.5)$, P3 $(-1.35, 2.0)$, P4 $(1.0, 2.0)$, P5 $(10.5, 2.0)$, P6 $(-0.5, 0.5)$, P7 $(1.0, 0.5)$ and P8 $(4.0, 0.5)$

$$d_2 = d_{2,n}^H = \frac{2(d_1 \tau \lambda_n + 1)(2d_1 \tau \lambda_n + \tau + 1)^2}{\theta \tau \lambda_n} > 0. \qquad (5.6)$$

Figure 3 shows the bifurcation diagram of system (5.4) in parameters $d_2$ and $\tau$, where $d_1 = 0.1$ and $\Omega = (0, \pi)$. For a fixed $\tau$, when $d_2$ varies from right to left starting from $d_2 = 0$, the constant equilibrium $(1, 1, 1)$ loses its stability at the first Turing bifurcation curve $d_2 = d_{2,n}^S(\tau)$ as defined in (5.5) to generate a spatial pattern; and similarly when $d_2$ varies from left to right starting from $d_2 = 0$, the constant equilibrium $(1, 1, 1)$ loses its stability at the first Hopf bifurcation curve $d_2 = d_{2,n}^H(\tau)$ as defined in (5.6) to generate a spatiotemporal pattern.

Again one can observe that when $\tau$ decreases, the dominant wave number $N$ (for steady-state bifurcation) or $M$ (for Hopf bifurcation) increases. When $\tau = 4.5$, the only possible spatial patterns are Turing type (Fig. 4 top row): the constant steady state is stable (see (a)) if $d_2 = -2.2 > d_{2,1}^S$, while mode-1 Turing patterns emerge if $d_2 = -2.5 < d_{2,1}^{lS}$ (see (b) and (c)). When $\tau = 2.0$, from the figures in the middle row of Fig. 4, one observes a spatially non-homogeneous mode-2 steady state at $d_2 = -1.35$, a homogeneous pattern at $d_2 = 1$, and a spatially non-homogeneous

**Fig. 4** Numerical simulations of system (5.4) when parameters are $d_1 = 0.1$ and $\Omega = (0, \pi)$. In each figure, the color indicates the value of $u(x, t)$ according to colorbar

mode-2 time-periodic pattern at $d_2 = 10.5$ (Fig. 4 middle row). For $\tau = 0.5$, similar sequence of patterns appear with mode-3 (Fig. 4 bottom row). One can also observe the spatially non-homogeneous time-periodic patterns at P5 or P7 are spatially and temporally periodic with expected spatial modes, and they are of "checker-board" type similar to the ones observed in the discrete delay version of spatial memory models in (Shi et al. 2019, 2020).

## 6 Discussion

In the past decade, spatial memory and cognition attracted much attention in the mechanistic modeling of animal movements (Morales et al. 2010; Fagan et al. 2013). We recently proposed a novel diffusive animal movement model with explicit spatial memory (Shi et al. 2020) by assuming that animals have information gained via their long-distance sight or social communications with their conspecifics (Schlägel and

Lewis 2014). Based on this recent work, we formulate a reaction–diffusion scalar equation with a distributed memory-based diffusion term to model the diffusive movement of animals who can memorize past information. In Shi et al. (2020), the memory-based diffusion is related to the memory of a particular moment in the past, which induces the discrete delay. It is also mentioned that a distributed delay for memory growing and decaying is more realistic since highly developed animals can remember the historic distribution or clusters of the species in space, but these spatial memories are decaying in their brains over time. Such decays may include decreases in intensity and spatial precision (Fagan et al. 2013; Shi et al. 2020). Therefore, this new distributed memory-based model (1.1) provides a more realistic quantitative framework for characterizing complicated memory waning and gaining processes in a relatively simple self-contained way.

The delay kernel plays a vital role in the modeling of distributed delay. In our case, we consider the spatial memory related to the memorized information during all the past times and the spatial distribution of the species. Thus, we need to choose proper delay kernels both in space and in time. For the spatial delay kernel, we use the Green's function of the diffusion equation that has been employed by many researchers to study the distributed delay effect (Gourley and So 2002; Chen and Yu 2016; Zuo and Song 2015). The temporal distribution of memory is modeled by the weak and strong kernel functions (two special cases of the Gamma distribution function) that have clear biological meanings. Under such settings, we transform the scalar population model (1.1) with the weak kernel into a two-species system (2.2) in which one of the "species" is the memory of the other one. Similarly, a three-species reaction–diffusion system (2.5) is obtained when the strong kernel is applied to the model. The method to establish the equivalence between the scalar reaction–diffusion equation with distributed delayed diffusion and reaction–diffusion system without delay is beneficial for us to gain a deep understanding of the original delayed model (1.1). Moreover, we prove that the eigenvalue problem of the original scalar Eq. (1.1) is exactly the same as the one for the equivalent system, which implies the equivalence of the stability of the constant steady state.

It is a pleasant surprise that Eq. (1.1) with the weak kernel is equivalent to the Keller–Segel chemotaxis model with growth (Keller and Segel 1970; Tello and Winkler 2007; Painter and Hillen 2011; Ma and Wang 2015), which means that another mechanism for this well-known model is established. In this case, the occurrence of steady-state bifurcations from the constant equilibrium can be theoretically proved, so non-homogeneous steady states exist. Through numerical simulations, we also observed spatially non-homogeneous time-periodic patterns. However, it is still an open problem to explain some drifting and wandering periodic patterns (see Fig. 2). For the strong kernel case, steady-state bifurcations and spatially non-homogeneous Hopf bifurcations from the positive constant equilibrium lead to spatially non-homogeneous steady states and non-homogeneous time-periodic patterns (see Fig. 4).

In our bifurcation analysis, we use the memory-based diffusion rate $d_2$ as the focused parameter. Also, we obtain the conditions for pattern formation: $d_2 < d_2^*$ for the weak kernel case and $d_2 \in (-\infty, d_{2,S}^*) \cup (d_{2,H}^*, +\infty)$ for the strong kernel case, which both satisfy $|d_2| > \theta d_1$, where $\theta$ is the positive constant steady state. Therefore, we can conclude that $|d_2| > \theta d_1$ is a necessary condition for pattern formation in system

(1.1). This result is consistent with the necessary condition obtained in Shi et al. (2020) for pattern formation of the discrete delayed spatial memory model. We also want to emphasize the significance of average time delay $\tau$ in the diversity of spatial patterns. From the bifurcation diagrams Figs. 1 and 3, we observe that the first bifurcation curve could be any mode as $\tau$ varies, which implies that diverse spatial patterns can emerge. In Fig. 4, it is clear that the spatial structure of the non-homogeneous steady states and time-periodic solutions is changing for different $\tau$ values.

Cognitive mapping is "a series of psychological transformations for acquiring, coding, storing, recalling and decoding spatial and attribute information in memory" (Fagan et al. 2013). We assumed a specific form of cognitive maps in our modeling efforts with explicit spatial memory. This heuristic model provides a simple self-contained theoretical framework for the future development of animal movement models with spatial memory. Our model can potentially be applied to quantitatively describe the spatiotemporal dynamics of animal movements in either terrestrial or aquatic ecosystems. It is natural to extend the modeling idea to interacting species in an ecosystem, for instance, spatial memory of resource distribution by consumers and spatial memory of predator distribution by prey. The aggregated research efforts in this direction will contribute to the ecological theory of cognitive animal movements.

# Appendix

***Proof of Theorem 3*** We apply Theorem 1.7 of Crandall and Rabinowitz (1971) for the local bifurcation. Fixing $d_1, \tau > 0$, we define a nonlinear mapping $F : \mathbb{R}^+ \times X^2 \to Y^2$ by

$$F(d_2, u, v) = \begin{pmatrix} d_1 \Delta u + d_2 div(u \nabla v) + f(u) \\ d_1 \Delta v + \frac{1}{\tau}(u - v) \end{pmatrix}. \tag{7.1}$$

It is clear that $F(d_2, \theta, \theta) = 0$ for any $d_2 > 0$. The Fréchet derivative of $F$ with respect to $(u, v)$ is

$$F_{(u,v)}\left(d_{2,n}^w, \theta, \theta\right)[\varphi, \psi] = \begin{pmatrix} d_1 \Delta \varphi + d_{2,n}^w \theta \Delta \psi + f'(\theta)\varphi \\ d_1 \Delta \psi + \frac{1}{\tau}(\varphi - \psi) \end{pmatrix} := L[\varphi, \psi]. \tag{7.2}$$

**Step 1.** First we determine the null space of $L$. From Lemma 4, we have $D_n(d_{2,s}^w) = 0$ so $\mu = 0$ is an eigenvalue of $J_n^w$ defined in (3.3) thus also an eigenvalue of (3.2) and there exists $q = (\varphi, \psi)^T = (1, h_n)\phi_n \in \mathcal{N}(L)$. Moreover as $T_n(d_{2,s}^w) > 0$, $\mu = 0$ is a simple eigenvalue of $J_n^w$; and since $\lambda_n$ is a simple eigenvalue of (1.4), and $d_{2,n}^w \neq d_{2,k}^w$ for any $k \in \mathbb{N}$ and $k \neq n$, then $\mu = 0$ is as simple eigenvalue of $L$ and

$$\mathcal{N}(L) = \text{Span}\left\{q = (1, h_n)\phi_n\right\},$$

with $h_n = 1/(d_1\lambda_n\tau + 1)$, thus dim $(\mathcal{N}(L)) = 1$.

**Step 2.** We next consider the range space $\mathcal{R}(L)$ of $L$. We can verify that $\mathcal{R}(L)$ is given by $\{(f_1, f_2) \in Y^2 : \langle q^*, (f_1, f_2)\rangle = 0\}$ where $q^* \in \mathcal{N}(L^*)$ and $L^*$ is the adjoint operator of $L$ and defined by

$$L^*[\varphi, \psi] = \begin{pmatrix} d_1\Delta\varphi + f'(\theta)\varphi + \frac{1}{\tau}\psi \\ d_1\Delta\psi + d_{2,n}^w\theta\Delta\varphi - \frac{1}{\tau}\psi \end{pmatrix}. \tag{7.3}$$

Since $\mathcal{N}(L^*) = \text{Span}\{q^* = (1, r_n)^T \phi_n\}$, where $r_n = \tau(d_1\lambda_n - f'(\theta))$. We obtain

$$\mathcal{R}(L) = \left\{ (f_1, f_2) \in Y^2 : \int_\Omega (f_1 + r_n f_2)\, \phi_n dx = 0 \right\},$$

and codim $(\mathcal{R}(L)) = 1$.

**Step 3.** We show that $F_{d_2(u,v)}(d_{2,n}^w, \theta, \theta)[q] \notin \mathcal{R}(L)$. From (7.1), we have

$$F_{d_2(u,v)}\left(d_{2,n}^w, \theta, \theta\right)[q] = (\theta h_n \Delta\phi_n, 0)^T = (-\theta\lambda_n h_n\phi_n, 0)^T. \tag{7.4}$$

Since

$$\int_\Omega (-\theta\lambda_n h_n\phi_n + 0)\, \phi_n dx = -\theta\lambda_n h_n \int_\Omega \phi_n^2 dx < 0,$$

thus $F_{d_2(u,v)}\left(d_{2,n}^w, \theta, \theta\right)[q] \notin \mathcal{R}(L)$ by the definition of $\mathcal{R}(L)$. From Step 1, 2 and 3, now we can apply Theorem 1.7 of Crandall and Rabinowitz (1971) to obtain part (i).

**Step 4.** Now we consider the bifurcation direction and stability of the bifurcating solutions in $\Gamma_n$. To obtain more detailed information of the bifurcation, we use one-dimensional domain $\Omega = (0, l\pi)$. In this case, it is known that $\phi_n = \cos(nx/l)$ and $\lambda_n = n^2/l^2$, so that $q = (1, h_n)^T \cos(nx/l)$. From Shi (1999), we have

$$d_{2,n}'(0) = -\frac{\langle l, F_{(u,v)(u,v)}(d_{2,n}^w, \theta, \theta)[q, q]\rangle}{2\langle l, F_{d_2(u,v)}(d_{2,n}^w, \theta, \theta)[q]\rangle},$$

where $l \in Y$ satisfies $\mathcal{N}(l) = \mathcal{R}(L)$ and can be calculated as

$$\langle l, (f_1, f_2)\rangle = \int_0^{l\pi} (f_1 + r_n f_2)\cos\left(\frac{nx}{l}\right) dx.$$

By (7.4) and the definition of $l$, we have

$$\langle l, F_{d_2(u,v)}\left(d_{2,n}^w, \theta, \theta\right)[q]\rangle = -\lambda_n h_n\theta \int_0^{l\pi} \cos^2\left(\frac{nx}{l}\right) dx = -\frac{\lambda_n h_n\theta l\pi}{2}.$$

From (7.1), it can be obtained that

$$F_{(u,v)(u,v)}(d_2, u, v)[\varphi, \psi][\varphi, \psi] = \left(2d_2\varphi'\psi' + 2d_2\varphi\psi'' + f''(u)\varphi^2, 0\right)^T. \tag{7.5}$$

This implies that

$$F_{(u,v)(u,v)} \left( d_{2,n}^w, \theta, \theta \right) [q, q] = \left( \frac{f''(\theta)}{2} + \left( \frac{f''(\theta)}{2} - 2 d_{2,n}^w h_n \lambda_n \right) \cos \left( \frac{2nx}{l} \right), 0 \right)^T,$$

(7.6)

and thus

$$\langle l, \ F_{(u,v)(u,v)} \left( d_{2,n}^w, \theta, \theta \right) [q, q] \rangle$$

$$= \int_0^{l\pi} \left( \frac{f''(\theta)}{2} + \left( \frac{f''(\theta)}{2} - 2 d_{2,n}^w h_n \lambda_n \right) \cos \left( \frac{2nx}{l} \right) \right) \cos \left( \frac{nx}{l} \right) dx = 0.$$

Therefore $d_{2,n}'(0) = 0$.

Next we calculate $d_{2,n}''(0)$ to determine the bifurcation direction by modifying the calculation in Jin et al. (2013). From Shi (1999), $d_{2,n}''(0)$ takes the form:

$$d_{2,n}''(0) = - \frac{\langle l, \ F_{(u,v)(u,v)(u,v)} \left( d_{2,n}^w, \theta, \theta \right) [q, q, q] \rangle + 3 \langle l, \ F_{(u,v)(u,v)} \left( d_{2,n}^w, \theta, \theta \right) [q, \Theta] \rangle}{3 \langle l, \ F_{d_2(u,v)} (d_{2,n}^w, \theta, \theta) [q] \rangle},$$

where $\Theta = (\Theta_1, \Theta_2)$ is the unique solution of

$$F_{(u,v)(u,v)} \left( d_{2,n}^w, \theta, \theta \right) [q, q] + F_{(u,v)} \left( d_{2,n}^w, \theta, \theta \right) [\Theta] = 0.$$

(7.7)

From (7.5), we have

$$F_{(u,v)(u,v)(u,v)} (d_2, u, v) [\varphi, \psi][\varphi, \psi][\varphi, \psi] = (f'''(u)\varphi^3, 0)^T,$$

thus

$$\langle l, F_{(u,v)(u,v)(u,v)} \left( d_{2,n}^w, \theta, \theta \right) [q, q, q] \rangle = \int_0^{l\pi} f'''(\theta) \cos^4 \left( \frac{nx}{l} \right) dx = \frac{3l\pi}{8} f'''(\theta).$$

(7.8)

In the following, we show the calculation of $\langle l, \ F_{(u,v)(u,v)} \left( d_{2,n}^w, \theta, \theta \right) [q, \Theta] \rangle$. By (7.6) and (7.7), we may assume $\Theta = (\Theta_1, \Theta_2)$ has the following form

$$\Theta_1 = \Theta_1^0 + \Theta_1^2 \cos \left( \frac{2nx}{l} \right), \quad \Theta_2 = \Theta_2^0 + \Theta_2^2 \cos \left( \frac{2nx}{l} \right),$$

(7.9)

since $F_{(u,v)(u,v)}\left(d_{2,n}^w, \theta, \theta\right)$ consists of only constant and $\cos\left(\frac{2nx}{l}\right)$ terms. Substituting (7.9) into (7.7), we obtain

$$
\begin{pmatrix}
-4d_1\lambda_n\Theta_1^2\cos\left(\frac{2nx}{l}\right) - 4d_{2,n}^w\theta\lambda_n\Theta_2^2\cos\left(\frac{2nx}{l}\right) + f'(\theta)\left(\Theta_1^0 + \Theta_1^2\cos\left(\frac{2nx}{l}\right)\right) \\
-4d_1\lambda_n\Theta_2^2\cos\left(\frac{2nx}{l}\right) + \frac{1}{\tau}[\Theta_1^0 - \Theta_2^0 + (\Theta_1^2 - \Theta_2^2)\cos\left(\frac{2nx}{l}\right)]
\end{pmatrix}
$$
$$
= -\left(\frac{f''(\theta)}{2} + \left(\frac{f''(\theta)}{2} - 2d_{2,n}^w\lambda_n h_n\right)\cos\left(\frac{2nx}{l}\right), 0\right)^T.
$$
(7.10)

Form Eq. (7.10), we can solve $\Theta$ as in (3.10). Thus, we obtain

$$
\begin{aligned}
&\langle l,\ F_{(u,v)(u,v)}\left(d_{2,n}^w, \theta, \theta\right)[q, \Theta]\rangle \\
&= 2d_{2,n}^w\lambda_n(\Theta_2^2 + h_n\Theta_1^2)\int_0^{l\pi}\sin\left(\frac{2nx}{l}\right)\sin\left(\frac{nx}{l}\right)\cos\left(\frac{nx}{l}\right)dx \\
&\quad + \left(f''(\theta) - d_{2,n}^w\lambda_n h_n\right)\Theta_1^0\int_0^{l\pi}\cos^2\left(\frac{nx}{l}\right)dx \\
&\quad + \left(f''(\theta)\Theta_1^2 - d_{2,n}^w\lambda_n h_n\Theta_1^2 - 4d_{2,n}^w\lambda_n\Theta_2^2\right)\Theta_1^2\int_0^{l\pi}\cos\left(\frac{2nx}{l}\right)\cos^2\left(\frac{nx}{l}\right)dx \\
&= \frac{l\pi}{2}d_{2,n}^w(\Theta_2^2 + h_n\Theta_1^2\lambda_n) + \frac{l\pi}{2}\left(f''(\theta) - d_{2,n}^w\lambda_n h_n\right)\Theta_1^0 \\
&\quad + \frac{l\pi}{4}(f''(\theta)\Theta_1^2 - 4d_{2,n}^w\lambda_n\Theta_2^2 - d_{2,n}^w\lambda_n h_n\Theta_1^2).
\end{aligned}
$$

Using all above we obtain $d_{2,n}''(0)$ in Eq. (3.9).

**Step 5.** By applying Corollary 1.13 and Theorem 1.16 of Crandall and Rabinowitz (1973) or Theorem 5.4 of Liu and Shi (2018), the stability of the bifurcating non-constant steady states can be determined by the sign of $\mu(s)$ which satisfies

$$
\lim_{s\to 0}\frac{-sd_{2,n}'(s)m'(d_{2,n}^w)}{\mu(s)} = 1,
$$
(7.11)

where $m(d_2)$ and $\mu(s)$ are the eigenvalues defined as

$$
F_{(u,v)}(d_2, \theta, \theta)[\varphi(d_2), \psi(d_2)] = m(d_2)K[\varphi(d_2), \psi(d_2)],
$$
$$
\text{for } d_2 \in (d_{2,n}^w - \epsilon, d_{2,n}^w + \epsilon),
$$
$$
F_{(u,v)}(d_{2,n}(s), U_n(s), V_n(s))[\Lambda(s), \Phi(s)] = \mu(s)K[\Lambda(s), \Phi(s)], \quad \text{for } s \in (-\delta, \delta),
$$

with $K : X \to Y$ is the inclusion map $K(u) = u$, $m\left(d_{2,n}^w\right) = \mu(0) = 0$ and $\left(\varphi\left(d_{2,n}^w\right), \psi\left(d_{2,n}^w\right)\right) = (\Lambda(0), \Phi(0)) = (1, h_n)\cos\left(\frac{nx}{l}\right)$.

Now consider the bifurcation at $d_2 = d_{2,N}^w = d_2^*$. From Lemma 4, $(\theta, \theta)$ is stable and $m(d_2) < 0$ when $d_2 > d_{2,N}^w$, and it is unstable and $m(d_2) > 0$ when $d_2 < d_{2,N}^w$.

One can calculate that

$$m(d_2) = \frac{-T_N + \sqrt{T_N^2 - 4D_N}}{2},$$

where $T_N$, $D_N$ are defined in (3.5), and this implies that $m'(d_{2,N}^w) = -\theta\lambda_N/(T_N\tau) < 0$. If $d_{2,N}''(0) < 0$, then $d_{2,N}'(s) < 0$ for $s \in (0, \delta)$ and $d_{2,N}'(s) > 0$ for $s \in (-\delta, 0)$. Hence $-sd_2'(s)m'(d_{2,N}^w) < 0$ for $s \in (-\delta, \delta)\backslash\{0\}$, and consequently $\mu(s) < 0$ by (7.11) and the bifurcating solutions are locally asymptotically stable. Similarly when $d_{2,N}''(0) > 0$, the bifurcating solutions are unstable. For any other bifurcation at $d_2 = d_{2,n}^w < d_2^*$, the trivial solution $(\theta, \theta)$ is already unstable at the bifurcation point, hence all bifurcating solutions are also unstable.

# References

Abrahms B, Hazen EL, Aikens EO, Savoca MS, Goldbogen JA, Bograd SJ, Jacox MG, Irvine LM, Palacios DM, Mate BR (2019) Memory and resource tracking drive blue whale migrations. Proc Natl Acad Sci 116(12):5582–5587

Amann H (1991) Hopf bifurcation in quasilinear reaction-diffusion systems. In: Delay differential equations and dynamical systems (Claremont, CA, 1990), volume 1475 of Lecture Notes in Mathematics. Springer, Berlin, pp 53–63

Bellomo N, Bellouquid A, Tao Y, Winkler M (2015) Toward a mathematical theory of Keller–Segel models of pattern formation in biological tissues. Math Models Methods Appl Sci 25(9):1663–1763

Britton NF (1990) Spatial structures and periodic travelling waves in an integro-differential reaction–diffusion population model. SIAM J Appl Math 50(6):1663–1688

Chen S, Yu J (2016) Stability analysis of a reaction–diffusion equation with spatiotemporal delay and Dirichlet boundary condition. J Dyn Differ Equ 28(3–4):857–866

Cooke KL, Grossman Z (1982) Discrete delay, distributed delay and stability switches. J Math Anal Appl 86(2):592–627

Crandall MG, Rabinowitz PH (1971) Bifurcation from simple eigenvalues. J Funct. Anal. 8:321–340

Crandall MG, Rabinowitz PH (1973) Bifurcation, perturbation of simple eigenvalues and linearized stability. Arch Ration Mech Anal 52:161–180

Ducrot A, Fu X, Magal P (2018) Turing and Turing–Hopf bifurcations for a reaction diffusion equation with nonlocal advection. J Nonlinear Sci 28(5):1959–1997

Fagan WF (2019) Migrating whales depend on memory to exploit reliable resources. Proc Natl Acad Sci 116(12):5217–5219

Fagan WF, Lewis MA, Auger-Méthé M, Avgar T, Benhamou S, Breed G, LaDage L, Schlägel UE, Tang WW, Papastamatiou YP, Forester J, Mueller T (2013) Spatial memory and animal movement. Ecol Lett 16(10):1316–1329

Fagan WF, Gurarie E, Bewick S, Howard A, Cantrell RS, Cosner C (2017) Perceptual ranges, information gathering, and foraging success in dynamic landscapes. Am Nat 189(5):474–489

Foss-Grant AP (2017) Quantitative challenges in ecology: competition, migration, and social learning. Ph.d thesis, University of Maryland

Golledge R (1998) Wayfinding behavior: cognitive mapping and other spatial processes. Johns Hopkins University Press, Baltimore

Gourley SA, Ruan S (2000) Dynamics of the diffusive Nicholson's blowflies equation with distributed delay. Proc R Soc Edinburgh Sect A 130(6):1275–1291

Gourley SA, So JW-H (2002) Dynamics of a food-limited population model incorporating nonlocal delays on a finite domain. J Math Biol 44(1):49–78

Hillen T, Buttenschön A (2020) Nonlocal adhesion models for microorganisms on bounded domains. SIAM J Appl Math 80(1):382–401

Hillen T, Painter KJ (2009) A user's guide to PDE models for chemotaxis. J Math Biol 58(1–2):183–217

Jin J, Shi J, Wei J, Yi F (2013) Bifurcations of patterned solutions in the diffusive Lengyel–Epstein system of CIMA chemical reactions. Rocky Mt J Math 43(5):1637–1674

Kappeler P (2010) Animal behaviour: evolution and mechanisms. Springer, Berlin, Heidelberg

Kareiva P, Odell G (1987) Swarms of predators exhibit preytaxis if individual predators use area-restricted search. Am Nat 130(2):233–270

Keller EF, Segel LA (1970) Initiation of slime mold aggregation viewed as an instability. J Theoret Biol 26(3):399–415

Kuto K, Osaki K, Sakurai T, Tsujikawa T (2012) Spatial pattern formation in a chemotaxis-diffusion-growth model. Phys D 241(19):1629–1639

Lee JM, Hillen T, Lewis MA (2009) Pattern formation in prey-taxis systems. J Biol Dyn 3(6):551–573

Lewis MA, Murray JD (1993) Modelling territoriality and wolf–deer interactions. Nature 366(6457):738–740

Liu P, Shi J (2018) Bifurcation of positive solutions to scalar reaction–diffusion equations with nonlinear boundary condition. J Differ Equ 264(1):425–454

Liu P, Shi J, Wang Z (2013) Pattern formation of the attraction-repulsion Keller–Segel system. Discrete Contin Dyn Syst Ser B 18(10):2597–2625

Ma M, Wang Z (2015) Global bifurcation and stability of steady states for a reaction–diffusion-chemotaxis model with volume-filling effect. Nonlinearity 28(8):2639–2660

Macdonald N (1987) Time lags in biological models: lecture notes in biomathematics, vol 27. Springer, Berlin

Mimura M, Tsujikawa T (1996) Aggregating pattern dynamics in a chemotaxis model including growth. Physica A 230(3–4):499–543

Moorcroft PR, Lewis MA (2006) Mechanistic home range analysis. Princeton University Press, Princeton

Moorcroft PR, Lewis MA, Crabtree RL (1999) Home range analysis using a mechanistic home range model. Ecology 80(5):1656–1665

Morales JM, Moorcroft PR, Matthiopoulos J, Frair JL, Kie JG, Powell RA, Merrill EH, Haydon DT (2010) Building the bridge between animal movement and population dynamics. Philos Trans R Soc B Biol Sci 365(1550):2289–2301

O'Keefe J, Nadel L (1978) The Hippocampus as a cognitive map. Oxford University Press, Oxford

Painter KJ, Hillen T (2011) Spatio-temporal chaos in a chemotaxis model. Phys D 240(4–5):363–375

Potts JR, Lewis MA (2016) How memory of direct animal interactions can lead to territorial pattern formation. J R Soc Interface 13(118):20160059

Potts JR, Lewis MA (2019) Spatial memory and taxis-driven pattern formation in model ecosystems. Bull Math Biol 81(7):2725–2747

Schlägel UE, Lewis MA (2014) Detecting effects of spatial memory and dynamic information on animal movement decisions. Methods Ecol Evol 5(11):1236–1246

Shi J (1999) Persistence and bifurcation of degenerate solutions. J Funct Anal 169(2):494–531

Shi J, Wang C, Wang H (2019) Diffusive spatial movement with memory and maturation delays. Nonlinearity 32(9):3188–3208

Shi J, Wang C, Wang H, Yan X (2020) Diffusive spatial movement with memory. J Dyn Differ Equ 32(2):979–1002

Shi J, Wang X (2009) On global bifurcation for quasilinear elliptic systems on bounded domains. J Differ Equ 246(7):2788–2812

Tao Y (2010) Global existence of classical solutions to a predator-prey model with nonlinear prey-taxis. Nonlinear Anal Real World Appl 11(3):2056–2064

Tao Y (2013) Global dynamics in a higher-dimensional repulsion chemotaxis model with nonlinear sensitivity. Discrete Contin Dyn Syst Ser B 18(10):2705–2722

Tello JI, Winkler M (2007) A chemotaxis system with logistic source. Commun Partial Differ. Equ. 32(4–6):849–877

Turing AM (1952) The chemical basis of morphogenesis. Philos Trans R Soc Lond Ser B 237(641):37–72

van Schaik CP (2010) Social learning and culture in animals. Springer, Berlin, pp 623–653

Wang Z, Zhao K (2013) Global dynamics and diffusion limit of a one-dimensional repulsive chemotaxis model. Commun Pure Appl Anal 12(6):3027–3046

Winkler M (2010) Boundedness in the higher-dimensional parabolic-parabolic chemotaxis system with logistic source. Commun Partial Differ Equ 35(8):1516–1537

Winkler M (2014a) Global asymptotic stability of constant equilibria in a fully parabolic chemotaxis system with strong logistic dampening. J Differ Equ 257(4):1056–1077

Winkler M (2014b) How far can chemotactic cross-diffusion enforce exceeding carrying capacities? J Nonlinear Sci 24(5):809–855

Winkler M (2017) Emergence of large population densities despite logistic growth restrictions in fully parabolic chemotaxis systems. Discrete Contin Dyn Syst Ser B 22(7):2777–2793

Wu S, Shi J, Wu B (2016) Global existence of solutions and uniform persistence of a diffusive predator-prey model with prey-taxis. J Differ Equ 260(7):5847–5874

Zuo W, Shi J (2021) Existence and stability of steady-state solutions of reaction–diffusion equations with nonlocal delay effect. Z Angew Math Phys 72(2):43

Zuo W, Song Y (2015) Stability and bifurcation analysis of a reaction–diffusion equation with spatio-temporal delay. J Math Anal Appl 430(1):243–261

Zuo W, Song Y Stability and double-Hopf bifurcations of a Gause–Kolmogorov-type predator-prey system with indirect prey-taxis. J Dyn Differ Equ 1–41 (to appear)

**Publisher's Note**  Springer Nature remains neutral with regard to jurisdictional claims in published maps and institutional affiliations.